

DIRECT BIOCONTROL OF TELEMANNIPULATORS AND VR ENVIRONMENTS
USING SEMG AND INTELLIGENT SYSTEMS

A Thesis

Presented to

The Graduate Faculty of the University of Akron

In Partial Fulfillment

of the Requirements for the Degree

Master of Science

Nikhil Shirao

May, 2006

DIRECT BIOCONTROL OF TELEMANIPULATORS AND VR ENVIRONMENTS
USING SEMG AND INTELLIGENT SYSTEMS

Nikhil Shirao

Thesis

Approved:

Accepted:

Dr. Narender P. Reddy
Advisor

Dr. Daniel B. Sheffer
Department Chair

Dr. Dale H. Mugler
Committee Member

Dr. George K. Haritos
Dean of the College

Dr. George C. Giakos
Committee Member

Dr. George R. Newkome
Dean of the Graduate School

Date

ABSTRACT

Virtual Reality describes a 3-D computer generated environment, controlled by the user from a remote location. VR has applications in robotics, entertainment and medical field. Virtual Reality robotic systems have been a major help in hazardous environments and in areas which need a high degree precision such as nuclear plants and tele-surgery. An ideal VR system immerses the user in the virtual environment. This condition is termed as telepresence. The components of a VR system are human operator, interface system and teleoperator. VR system relies on human interface performance for its high accuracy. Commercially available interfaces such as Data Gloves and exoskeleton devices provide less accuracy and restricted motion. A biocontrol interface utilizing human physiological signals such as Electromyogram (EMG) would be a natural and synergistic way of controlling a remote teleoperator.

Previous studies (Suryanarayan and Reddy) have shown that surface EMG (SEMG) from flexor muscle can be effectively used as a human interface for controlling teleoperators for dynamic motion of elbow joints. The goal of the present study was to investigate the use of SEMG from extensor muscle to control real time dynamic movement of index finger at various speeds for full range. Normal subjects were asked to rhythmically flex and extend the index finger at different speeds. The actual angle was measured using a miniature accelerometer. SEMG from extensor muscle (Extensor

Digitorum Superficialis (EDS)) was used to correlate with angle made by index finger at various speeds, with all other fingers at constant position. Parameters were extracted from SEMG. Neural networks were trained with input as extracted parameters and targets as measured angles. Best five networks were recruited for each committee. Two committees for each speed were formed. The committees were evaluated using data from new subject and the errors between actual and predicted joint angle was calculated.

The committees were able to predict the joint angle at different speeds. The RMS errors between the predicted and the actual angle were found to be between 3-27%. The errors were more in the flexion region as compared to the extensor region. The study demonstrated the use of SEMG from EDS for the prediction of joint angle at different speeds. It also demonstrated the use of committee neural networks (CNN) in control related prediction problems. The study has taken a step forward in the direct biocontrol of telemanipulator and VR environments using SEMG. The study would find an application in medicine and control of robotic assist devices.

ACKNOWLEDGEMENTS

I would like to express my sincere and deepest gratitude to my advisor Dr Narender Reddy for his constant support, guidance and encouragement. Without him, this project would have been a distant possibility. I would also like to thank my committee members, Dr Dale Mugler and Dr George Giakos for kindly agreeing to be the part of my committee. Their advice and suggestions have been valuable in making this project a success.

I would also like to thank the faculty of the Department of Biomedical Engineering for their support and encouragement. I would like to thank Rick Nemer, for constantly helping me with my hardware problems. A special mention goes to Russ Humn for providing me the right direction when I was stuck with my hardware.

The project would be incomplete without the mention of my lab partner Renu. She was always by my side throughout the project, constantly giving me encouragement and new ideas and was a source of motivation, I owe a lot of success of this project to her. I would like to thank my friends Lakshmi and Nemath for their support and help not only in the project but throughout my stay in the University

Last but not the least, I would like to thank my parents for their constant love, support and encouragement. My deepest gratitude goes to them for constantly standing by me and exemplifying their faith in my abilities. Thank you Papa. Thanks Mom.

TABLE OF CONTENTS

	Page
LIST OF TABLES.....	ix
LIST OF FIGURES.....	x
CHAPTER	
I INTRODUCTION.....	1
II LITERATURE REVIEW.....	6
2.1 Virtual Reality.....	6
2.2 Telepresence.....	7
2.3 Telesurgery.....	8
2.4 Interfacing Devices.....	10
2.4.1 Cyber Gloves.....	11
2.4.2 Magnetic Trackers.....	11
2.4.3 Optical Position Tracking System.....	12
2.4.4 External Skeletal Devices.....	12
2.5 Anthropomorphic Telemanipulator.....	13
2.6 EMG.....	14
2.7 EMG Analysis.....	16
2.8 Choice of the muscle.....	19

2.9 Neural Networks.....	20
2.9.1 Transfer Functions.....	24
2.9.2 Learning Process.....	26
2.9.3 Back Propagation.....	29
2.9.4 Applications of Neural Networks.....	29
III METHODOLOGY.....	32
3.1 Instrumentation.....	34
3.1.1 Differential Preamplifier.....	34
3.1.2 Amplifier.....	35
3.2 Location and Placement of Electrodes.....	35
3.2.1 Placement of Reference Electrode.....	39
3.3 Choice of Subjects.....	39
3.4 Protocol.....	39
3.5 Data Acquisition.....	41
3.6 Signal Processing.....	41
3.6.1 Processing of SEMG Signals.....	44
3.6.1.1 RMSEMG.....	44
3.6.1.2 Filtration.....	44
3.6.1.3 Calibration Calculations.....	44
3.6.1.4 Normalization of the signal.....	45
3.6.2 Parameters Extraction.....	45
3.7 Processing of Accelerometer Data.....	46

3.7.1	Determination of the Angle from Accelerometer Voltages....	48
3.7.2	Accelerometer Calibration.....	48
3.8	Development and Training of Neural Network.....	49
3.9	Analysis of the Results.....	53
IV	RESULTS.....	54
4.1	Results from Data Acquisition.....	54
4.2	Results from CNN.....	58
4.3	Statistical Analysis.....	77
V	DISCUSSION.....	82
VI	CONCLUSION AND FUTURE WORK.....	91
6.1	Conclusion.....	91
6.2	Recommendations for the Future Work.....	92
	REFERENCES.....	93
	APPENDICES.....	98
	APPENDIX A ACCELEROMETER READINGS.....	99
	APPENDIX B STATISTICAL ANALYSIS.....	100
	APPENDIX C IRB APPROVAL.....	102
	APPENDIX D INFORMED CONSENT.....	103

LIST OF TABLES

Table		Page
3.1	Technical Specifications of the System.....	36
3.2	Accelerometer Specifications.....	50
4.1	RMS Errors of CNN Prediction.....	81

LIST OF FIGURES

Figure	Page
2.1 Architecture of A Telesurgical System.....	9
2.2 Raw EMG of the Subject Taken from FDS.....	17
2.3 McCulloch and Pitts Model Neuron.....	23
2.4 Typical Two Layer Neural Network.....	25
2.5 Input and Output Relation in a Sigmoid Transfer Function.....	27
3.1 Overall Flowchart of the Methodology.....	33
3.2 Block Diagram of the Instrumentation System.....	37
3.3 Location and Placement of the electrodes on the posterior forearm of the subject.....	38
3.4 Full Extension Position of the Index Finger.....	42
3.5 Full Flexion Position of the Index Finger.....	43
3.6 Block Diagram of the Data Acquisition System.....	47
3.7 Plot of Voltage Output of the Accelerometer Vs Angle.....	52
4.1 Raw SEMG from EDS when the Subject was Performing Rhythmic Flexion and Extension of the Index Finger at 0.4 Hz.....	55
4.2 Raw SEMG from EDS when the Subject was Performing Rhythmic Flexion and Extension of the Index Finger at 0.8 Hz.....	56
4.3 Raw SEMG from EDS when the Subject was Performing Rhythmic Flexion and Extension of the Index Finger at 1.2 Hz.....	57

4.4	Plot of Filtered RMS SEMG Vs Time for 0.4 Hz.....	59
4.5	Plot of Accelerometer Values Vs Time for 0.4 Hz.....	60
4.6	Plot of Angles Vs Time for 0.4 Hz.....	61
4.7	Plot of Normalized SEMG Vs Normalized Angles for 0.4 Hz.....	62
4.8	Plot of Shifted NRMS Vs Normalized Angles for 0.4 Hz.....	63
4.9	Plot of Filtered RMS SEMG Vs Time for 0.8 Hz.....	64
4.10	Plot of Accelerometer Values Vs Time for 0.8 Hz.....	65
4.11	Plot of Angles Vs Time for 0.8 Hz.....	66
4.12	Plot of Normalized SEMG Vs Normalized Angles for 0.8 Hz.....	67
4.13	Plot of Shifted NRMS Vs Normalized Angles for 0.8 Hz.....	68
4.14	Plot of Filtered RMS SEMG Vs Time for 1.2 Hz.....	69
4.15	Plot of Accelerometer Values Vs Time for 1.2 Hz.....	70
4.16	Plot of Angles Vs Time for 1.2Hz.....	71
4.17	Plot of Normalized SEMG Vs Normalized Angles for 1.2 Hz.....	72
4.18	Plot of Shifted NRMS Vs Normalized Angles for 1.2 Hz.....	73
4.19	NRMS Vs Normalized Angles for 0.4 Hz.....	74
4.20	NRMS Vs Normalized Angles for 0.8 Hz.....	75
4.21	NRMS Vs Normalized Angles for 1.2 Hz.....	76
4.22	NRMS, Actual Normalized Angle and Predicted Normalized Angle Plotted against Time at 0.4 Hz.....	78
4.23	NRMS, Actual Normalized Angle and Predicted Normalized Angle Plotted against Time at 0.8 Hz.....	79
4.24	NRMS, Actual Normalized Angle and Predicted Normalized Angle Plotted against Time at 1.2 Hz.....	80

CHAPTER I

INTRODUCTION

Robotic telemanipulators and Virtual Reality (VR) have seen many rapid advances in the recent times. A VR environment is defined as a 3-D computer world that looks and feels real. During last few decades, VR has made its presence felt in many areas, including combat simulation, virtual flight simulation, rehabilitation (Reddy et. al, 1994) and entertainment. A lot of interest has been generated in controlling a mechanical device or a telemanipulator from a remote environment. A telemanipulator can be used in potential hazardous environments, video games, rehabilitation, space and military. It gives the operator the capacity to manipulate real world environments from the comfort of his/her workplace. Robotic telemanipulators have been used in assisting surgical procedures such as endoscopy and image guided surgeries for brain tumor. The advances in robotic telemanipulators have the potential to make complex surgical procedures minimally invasive, reducing the time and effort for the procedure, and increasing the efficiency of the operator by many fold. It is extremely important that the tasks performed by the robotic manipulator closely follow the behavioral pattern of the operator, both intellectually and anatomically. The system should also be able to provide a haptic and visual feedback to make the operator feel present, and immersed in the environment. This condition is termed as telepresence.

The components of an ideal telemanipulator system are:

- Human Operator, which controls the environment from a remote location.
- Teleoperator, which is a remote operator controlled by the human and,
- Interfacing device, which acts as data transfer system between the operator and the telemanipulator.

The performance of the overall systems is dictated by the performance of its subsystems, and any errors in any of the subsystem can translate into the erroneous operation of the entire system. A teleoperator, which has anatomical structures matching the human, is termed as an anthropomorphic telemanipulator. The interfacing devices can take the form of human features, such as data glove, or device which assist the human operations, such as joy sticks and key boards. An interfacing device is responsible for transferring the manipulation information from the operator to the teleoperator as well as feedback information from the teleoperator to the operator. However, the development of an ideal interfacing device, which could reliably transfer the information both ways, has always posed problems for researchers.

Some of the commercially available devices include joy sticks, magnetic trackers, DataGloveTM, CyberGlove®, Exo-Skeletal devices (EXOS), motion trackers such as Flock of Birds (Ascension Inc.) and ultrasound trackers. These devices measure the joint angle of fingers or the position of the operating anatomical structure. Even though these devices are used for controlling a telemanipulator, they have several limitations. DataGloveTM measure the angle and position of the finger using several resistors. However, the accuracy of the measurement depends on the position of the resistors on the

human hand, which varies with the size and structure of the human hand, inducing error in the system. Moreover, the calibration procedures of DataGloveTM are complicated and static errors are in the range of 4-8° (Burdea and Langarana, 1992). Furthermore, these errors were obtained on mechanical models not using the actual finger joints. EXOS are very bulky and hence cause fatigue to the user, thus compromising the ability of the user to work in stressful environments.

Therefore, there is a need to develop an interfacing device which would overcome these problems, while maintaining the required accuracy of the system. The system should be very easy to calibrate, and should not cause a hindrance to the natural working habits of the user. Direct bio-control of the telemanipulator using physiological signals such as Electro-oculogram (EOG) and Surface Electromyogram (SEMG) can provide a useful control of the telemanipulator, thus making the system more synergistic and natural. Out of all the physiological signals, SEMG presents the most useful information about the movement and the activity of the user, and can be used to control an anthropomorphic telemanipulator. The SEMG is random, non stationary and non-linear (Duchene, 1993) and is the manifestation of the electrical activity of the human muscle. A lot of study has been conducted in studying the relation between SEMG and the muscle activity (Kearney, 1990). But most of the studies have investigated the isometric properties of the muscle, and failed to address the dynamic movements of the limb. The SEMG signal pattern for the dynamic movement of the limb depends on several factors, such as the velocity of the muscle movement, load on the muscle and the time for which the activity is performed. Also, the nature of the SEMG varies with environmental factors

such as temperature, humidity, measurement conditions, skin impedance and the placement of electrodes. A change in any of these factors may result in unpredictable change in the SEMG pattern.

Attempts have been made to study the usefulness of the SEMG for the control of a telemanipulator. Reddy and Gupta (2006) used SEMG from flexor muscles to control computer models of finger and wrist. However, their study was limited to 24° of finger flexion, from neutral position to touching the thumb. Moreover, the study involved only static analysis. Previous studies conducted by Suryanarayan and Reddy (1997), on dynamic tracking of elbow joint movement using the SEMG, showed that the SEMG can be used for the control of the telemanipulator. The non-linear nature of the signal prompted them to use hybrid intelligent systems involving neural networks and fuzzy logic. Devavaram (2003) conducted the investigation on the dynamic movement of the finger by acquiring the SEMG from flexor muscle. However, the range of the investigation was limited to 20° flexion of the finger. The study made use of individual committee neural network for each subject, making the procedure very cumbersome and complicated. The question still remains whether the SEMG can be used to predict the joint angle of the finger for the entire range of flexion and extension at various speeds. The present investigation was aimed at answering this question. Specific objectives of the study were:-

- To develop a reliable SEMG signal acquisition system for acquiring SEMG signals from Extensor Digitorum Superficialis muscle (EDS), during the movement of index finger at various speeds.

- To acquire SEMG signals from subjects at various speeds, during the flexion and extension of index finger.
- To find a relation between strength of the SEMG signal and joint angle.
- Extract parameters from the SEMG for the training of neural networks.
- Train Artificial Neural Networks (ANN) for the prediction of joint angle of the finger rotation.
- Recruit the committee for the prediction of joint angle.
- Evaluate the result by finding RMS errors between the predicted angle and actual angle measured by accelerometer.

The hypotheses of the study are:

Null Hypotheses

1. There does not exist a definite relation between the SEMG from EDS muscle and the joint angle of the finger movement at various speeds.
2. SEMG along with Committee Neural Networks (CNN) cannot be used for predicting the joint angle of the finger movement at various speeds (average RMS errors >0.2).

Alternate Hypotheses

1. There exists a definite relation between the SEMG from EDS muscle and the joint angle of the finger movement at various speeds.
2. SEMG along with Committee Neural Networks (CNN) can be used for predicting the joint angle of the finger movement at various speeds (average RMS errors <0.2).

CHAPTER II

LITERATURE REVIEW

2.1 Virtual Reality

Virtual Reality (VR) addresses as many human senses as possible. The term Virtual Reality describes a computer-generated scenario of objects (virtual world) the user can interact with. In contrast to conventional man-computer interfaces, the interaction is designed in three dimensions rather than two. The combination of three-dimensional computer graphics, special display techniques (head mounted display or stereo glasses) and specific input devices (spaceball, CyberGlove®, etc) allow intuitive manipulation of objects in the virtual world, thus giving users the impression of being part of the world.

Sutherland (1965) described Virtual Reality, as a looking glass into the mathematical wonderland, constructed in the computer memory. He coined the idea of an ultimate display, where the existence of matter is controlled by the computer (Sutherland, 1965). Virtual Reality, since then has seen many advances. Its use covers a wide range of spectrum ranging from military to medical. Some of the most common applications of VR are aircraft simulators, surgical simulators, telepresence systems and teleoperations. In 1985, NASA scientists and engineers at Ames Research Center in Palo Alto, California, used VR techniques for developing a Martian environment for training their

space missions. This event marked the beginning of the use of VR for scientific visualization. The use of VR in medicine started with its application in medical education. Medical applications in VR include telepresence surgery, 3-D visualization of human anatomy and VR surgical simulators (Satava, 1995). Numerous surgical simulators in the field of ophthalmology, laproscopy, urology, orthopathy and neurologic surgery are presently in use. These simulators are mainly used in teaching cognitive and manual skills (Zajtchuk and Satava, 1997). NASA scientists at Johnson Space Center, in collaboration with the University of Texas Medical Branch at Galveston and the Galveston Independent School District, developed a Virtual Visual Environmental Display (VIVED). This is a high resolution simulator for human body and is used for educational purposes (Suzanne, 1994).

2.2 Telepresence

The cardinal concept to define a VR system in terms of human experience is presence. Gibson (1979) described presence as perception of one's surroundings, generated by an automatic and controlled mental process, and not as one's surrounding in the physical world. The user should be totally immersed in the environment and should feel a sense of telepresence.

The different factors, which influence the sense of presence, are the inputs from some or all sensory channels and the mental process that integrates the data to give it a real meaning based on past experiences (Gibson 1966). Researches have been trying to incorporate these factors to make a VR system appear more real. In a telepresence system

the user has all the necessary inputs which make him feel to be present at the site of operation. Applications of telepresence include Entertainment and Telesurgery.

2.3 Telesurgery

Telesurgery is an important application of telepresence and is gaining importance in teleoperations. Telesurgical manipulations are used in battlefields and in emergency surgical operation situations. Surgeons have started making use of telesurgery in urology. A robotic laparoscopy surgery provides many advantages over a conventional laparoscopy, such as stereovision, dexterity and tremor filtering. However, such kind of surgery requires a lot of practice on the part of surgeon, mainly because of magnification and lack of tactile feedback (Rassweiler et. al, 2001). Further, although the current systems offer numerous advantages, the principal paradigm remains the same, and that is manual control of the instruments with visual feedback by video cameras. Figure 1 shows the general architecture of a telesurgical system.

A Telesurgical system consists of following constituents:

1. Human Operator
2. Interfacing Devices
3. Computer Networks and Data Processing Systems
4. Patient Database and Treatment Module
5. Anthropomorphic Teleoperator

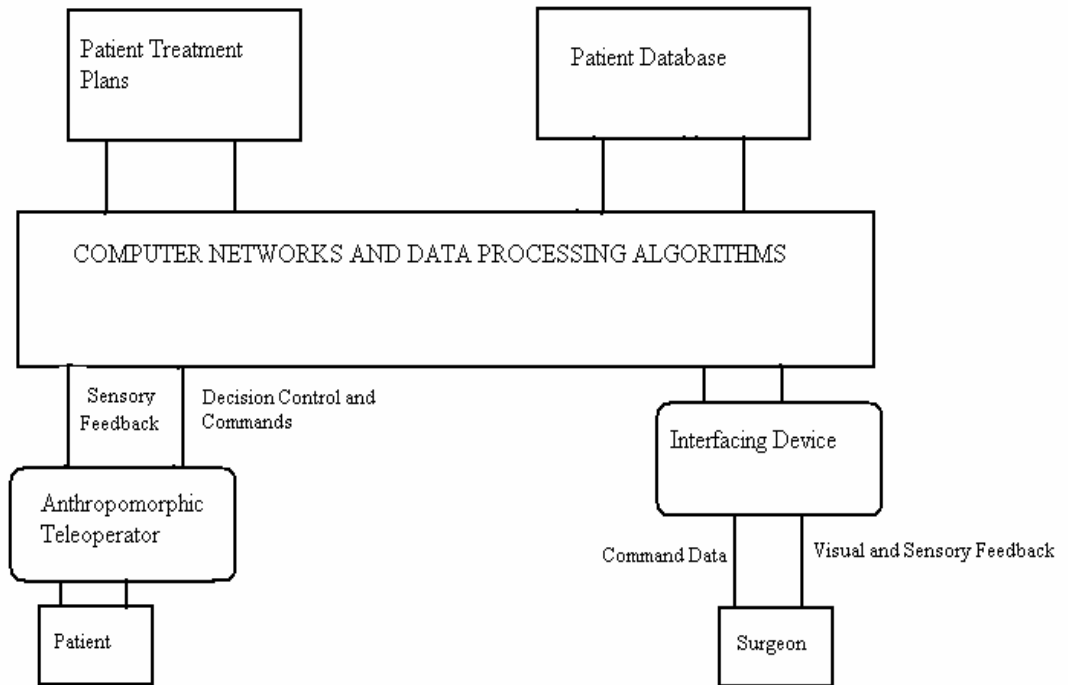


Figure 2.1. Architecture of a Telesurgical System

2.4 Interfacing Devices

The control data from the operator is acquired by an interface device, which plays an important part in a teleoperations system. The interface device is responsible for transmitting physiological data to the control system in a form that can be used for controlling the telemanipulator located at a remote site, or to interact with the VR environment. The overall performance of the telemanipulator system is largely dictated by a reliable, robust and error free interface device. The first modern master-slave teleoperator system was developed by Raymond Govertz in 1940, at Argonne National Laboratory near Chicago, for manipulation of radioactive materials. Since then, interfacing devices have seen a lot of technological advances in the field of space, military, mining and telesurgical operations. Sutherland in 1968 developed the first head mounted display which measured the viewing direction. Advanced naval systems use cable and video cameras to control teleoperators on submarines. Several commercial systems are available for the use in human interface for teleoperations. Commercial interfaces for tracking human arm movements include CyberGlove®, joy sticks, magnetic and ultrasound trackers, Optical Position Tracking System (OPTS), power gloves, external skeletal devices etc. Although these systems offer a definite advantage over humans, they suffer from various performance disadvantages which are discussed in the proceeding section.

2.4.1 CyberGlove®

A CyberGlove® is mounted with series of flexible sensors for measuring the position of the finger and the wrist. A CyberGlove® makes use of the bend sensor for sensing the motion. The sensors measure the resistance generated due to bending. This change in resistance gives the measure of the degree of motion. These gloves are widely used for sensing finger motions, but they have a serious limitation associated with them. The sensor is prone to environmental noise resulting in the tremor in virtual hand. A repeatability evaluation study conducted by Dipietro et. al (2003) on a 20 DOF human glove showed an overall performance error of 6.17°. Though the system offered many advantages over the conventional data gloves like more number of sensors for measurement (20) as compared to data gloves (10) and ability to measure abduction due to increased sensors, it lacked the required repeatability in telesurgery. Furthermore, the repeatability error increases for humans with different anatomical hand structure. Dipietro et. al (2003) reported that the system performance is acceptable in rehabilitation but the cost of the system may be a hinder for its widespread use. It is also difficult to implement haptic feedback control due to the presence of glove (Dipietro et. al, 2003).

2.4.2 Magnetic Trackers

Magnetic trackers, also called as “Flock of Birds” was developed by Scully in 1993. The system is an assembly of receivers and transmitters, using alternate low-frequency field to determine an object’s motion. Magnetic trackers use sets of coils that are pulsed to produce magnetic fields. The magnetic sensors determine the strength and

angles of the fields. Limitations of these trackers are, a high latency for the measurement and processing, range limitations, and interference from ferrous materials within the fields.

2.4.3 Optical Position Tracking System (OPTS)

Optical Position Tracking System (OPTS) was developed as an alternative to magnetic trackers. OPTS makes use of a ceiling LEDs grid, which emit the light in pulse sequences, and a head mounted camera. The camera's image is processed to detect the flashes. The problems with this method are, limited space (grid size) and lack of full motion (rotations). Another optical method uses a number of video cameras to capture simultaneous images that are correlated by high speed computers to track objects. The processing time of the image is a major limiting factor here along with the cost of high speed image processing hardware.

2.4.4 External Skeletal Devices (EXOS)

An Exo-skeletal Device is a metallic structure worn at the back of the hand. A typical exo-skeletal device is made up of rotatory potentiometers to measure the position of fingers and hand.

There are several problems associated with the system, such as large size causing tiredness to the user, and limitations to the natural fingers operation. The device also ranks low on the accuracy measure due to the position of the sensors. The sensors

are not placed on the joints causing a high degree of inaccuracy in the measurement. The wire used for haptic feedback suffers from friction, expansion and contraction thus compromising the accuracy of the measurements (Tatsuya et. al, 2002).

2.5 Anthropomorphic Telemanipulator

The most important criteria for an ideal teleoperator system is the dexterity of the telemanipulator. In order to control the remote environment, the actions of the human operator should be exactly copied by the telemanipulator system. Such kind of telemanipulator is called as an anthropomorphic telemanipulator (Sheridan, 1992). A telemanipulator provides the necessary input to the user to remotely control the environment. It would sense the environment with sensors resembling eyes (e.g. camera), manipulate objects by mechanical arms that resemble hands and move with parts resembling legs.

Anthropomorphic telemanipulator has wide-ranging applications in the field where a human operator cannot perform with high degree of effect, and where the safety of a human operator can be compromised, such as nuclear reactors, mining and military operations. Some of the applications of an anthropomorphic telemanipulator include surgical simulations and telesurgery.

The overall performance of the telesurgery system is largely dictated by a reliable, robust and error free human interface device. However, all of the mentioned systems have several drawbacks including rigid command configuration, limited range of activity, inconvenient to use during long hours of operations and susceptibility to external

noise. Bio-control of the telemanipulator involving physiological signals like Electroencephalograph (EEG), Electro-oculograph (EOG) and Electromyograph (EMG) is thought to be an alternative and very useful way of eliminating most of the drawbacks of commercially available systems. Electro-oculograph (EOG) is an electrical signal generated by the vertical and horizontal eye movements. However, the use of EOG is limited to vision based control of telemanipulators. Also, the utility value of an EOG signal is limited because of its low range of information content and uneasiness to the user. EEG represents electrical activity of the brain. Several researchers have attempted to track brain functions using EEG signals, but due to extreme complexity of the signal, they were able to achieve only a two stage control in a much selected subject population. Electromyograph on the other hand is a direct representation of the muscle activity and hence is the most natural signal for the synergetic control of the telemanipulator systems. Out of these physiological signals, EMG is the most promising and maybe the most appropriate for controlling an anthropomorphic teleoperator.

2.6 EMG

The myoelectric signal is the electrical manifestation of the neuromuscular activation associated with a contracting muscle. The myoelectric signal is an extremely complicated signal. It is greatly affected by the anatomical and physiological properties of the muscles and the control scheme of the peripheral nervous system. The quality of detection of a myoelectric signal largely depends on the characteristics of the instrument that is used to detect and observe the signal (De Luca, 1979). The electrical activity can

be measured by using either needle electrodes (Palmer et. al, 1991; Perlman et. al, 1989) or surface electrodes (Gupta et. al, 1996). Needle electrodes are used to measure the electrical activity of specific muscle, while surface electrodes are used to measure the gross activity from a group of muscles. The electrical activity measured is called electromyograph. The amplitude of the EMG is the resultant integration of all electrical activities of a muscle at a particular instant of time (Cromwell et. al, 1980). The amplitude of EMG is stochastic in nature and can be reasonably represented by a Gaussian distribution function. The amplitude of the signal can range from 0 to 10 mV (peak to peak) or 0 to 1.5 mV (RMS) (Carlo J. De Luca, 2002). The useful energy of EMG is limited to the range of 30 to 300 Hz. EMG is currently used for several applications such as

- Kinesiology: To monitor muscle function performance
- Gait Analysis
- Biomechanics: To monitor the muscle activities during movement
- Myoelectric control of prosthesis
- Rehabilitation
- Diagnosis of neuromuscular disorders

EMG is the result of the contractions of the muscle, and the basic structural unit of contraction is a muscle fiber. The fibers always contract in group and the collective contraction of these muscle fibers produces resultant EMG. The muscle fibers are supplied by the terminal branches of one nerve fiber, whose cell body is in the anterior horn of the spinal grey matter. These muscle fibers, along with the innervating axon

running down the motor nerve and its terminal branches, constitute a motor unit. The number of fibers innervated by a single motor unit differs according to the location of muscle. Generally, muscles controlling fine movements have smallest number of muscle fibers per motor unit (e.g. Muscles of eyeball or larynx). On the other hand, coarse acting muscles have larger number of muscle fibers per motor unit. The contraction of a voluntary muscle is under the control of nerves and they contract only when the nerve impulse reaches the muscle. The contraction of a muscle is all or none phenomenon i.e., so long as stimulation is sufficient to cause a contraction, there is only one degree of contraction and that is maximal. When an impulse reaches the motor endplate, a wave of contraction spreads over the fiber resulting in a brief twitch, followed by rapid and complete relaxation. The duration of the twitch and relaxation varies from few msec to 0.2 secs. The muscle fibers of a motor unit do not contract at the same time, and hence the electrical potential developed by a single twitch of all the fibers in the motor unit is prolonged to about 5 to 12 msec (Guyton, 1971). Figure 1.2 shows the plot of the raw SEMG taken from the Flexor Digitorum Superficialis (FDS) of the subject when the index finger was relaxed.

2.7 EMG Analysis

EMG signals have been a very effective research tool since decades. Sukhtankar and Reddy (1993) used SEMG to control Finite Element Models of hand. The EMG is extensively used for muscle function assessment, pathology identification and pattern classification (Duchene and Goubel, 1993). Farry et. al (1995) have shown that EMG

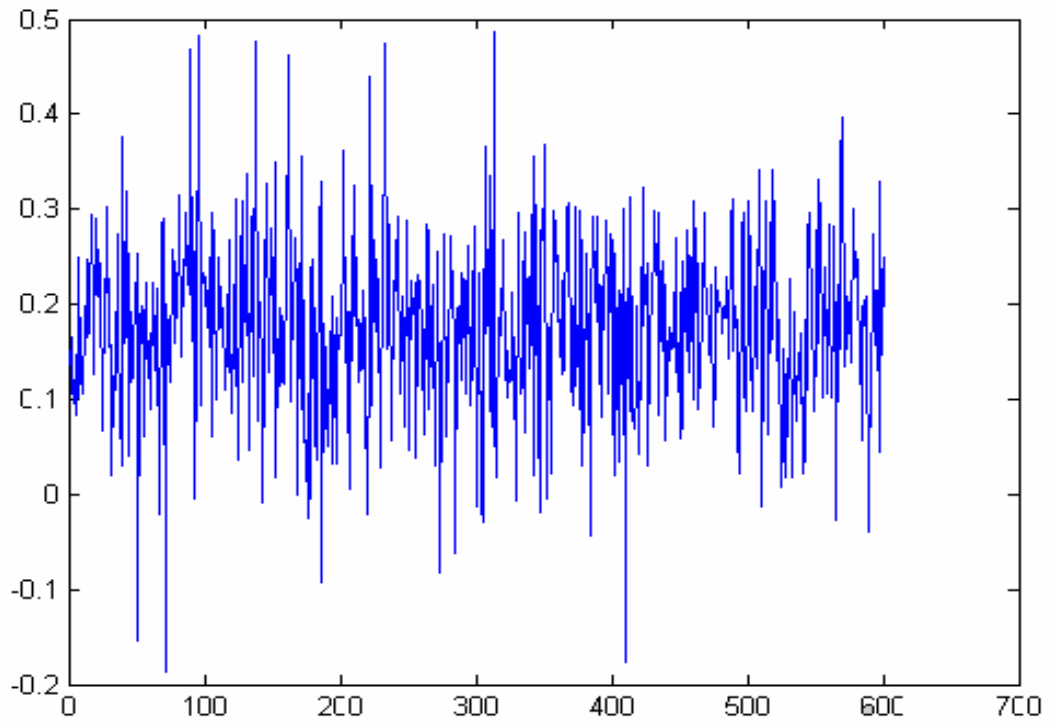


Fig 2.2 Raw EMG of the subject taken from Flexor Digitorum Superficialis and filtered at 30-300 Hz.

can be used for the teleoperation of a complex anthropomorphic robotic hand, by converting the myoelectric signal into robot commands replicating the motion. Their research used EMG for switching on pre-programmed motions of the robotic hand, such as chuck and key grasp primitives. Since, the motions were pre-programmed therefore, the operator had limited freedom in the use of this technique.

Other researches such as Utah/MIT dexterous hand (Jacobsen et. al, 1986) have used EMG to design a 4-DOF robotic finger and 4-DOF robotic thumb. EMG signals have often been used as control signals for prosthetic hands. Wiener (1948) proposed the concept of an EMG- controlled prosthetic hand. EMG signals have been used as control signals for prosthetic hands such as Waseda hand (Kato et. al, 1967) and Boston arm (Jerard et. al, 1974).

However, these prosthetic hands are seldom used by the amputees for two main reasons. First, the hardware device has problems such as motor noise and excessive weight. Second, there is a problem of interfacing the human and the device (Fakuda et. al, 2002).

EMG signals have been analyzed either in time or the frequency domain to characterize the muscle activity (Merletti and LaConte, 1995). Bilodeau et. al (1992) performed time and frequency analysis of EMG signals of homologous elbow flexors and extensors. Power spectral analysis has been performed in the frequency domain on the EMG signals to determine the frequency pattern of the signal in normal and pathologic muscles (Ronager et. al, 1989). EMG signals have been high pass, low pass and band pass filtered to eliminate the effect of noise (Kenemans et. al, 1991).

Surface EMG is a direct result of the muscle activities and therefore, considered to be the most useful physiological data to be used in a bio-control interface. However, the relation between EMG and arm dynamics in the presence of motion has not been fully understood. The EMG signal pattern depends on several factors such as velocity of movement, amplitude of movement, position of the arm and the condition of the subject. Recent studies by Suryanarayan and Reddy (1997) have successfully employed the use of surface EMG from the biceps muscle to predict the joint angle of the elbow at different speeds. Gupta (1997) have used SEMG from the FDS muscle and the Flexor Carpi Ulnaris (FCU) muscle to manipulate anthropomorphic computer models of two fingers and wrist teleoperators at constant speed. However, the pattern of surface EMG is also affected by the velocity of the movement. Therefore, the question remains whether SEMG can be used to accurately predict the finger angle at different speeds. The purpose of the research was to address this question.

2.8 Choice of the muscle

Preliminary experiments and previous studies have shown that the SEMG acquired from the Extensor Digitorum Superficialis (EDS) shows better linearity when plotted against the joint angle of the index finger, as compared to the SEMG from the FDS muscle and the FCU muscle, during the motion of the index finger. Therefore, in the present study we made use of EDS for gathering the SEMG for rhythmic flexion and extension of the index finger. The EDS arises from the common extensor origin on the anterior aspect of the lateral epicondyle of the humerus. It occupies most of the posterior

region of the forearm. It divides into four tendon slips proximal to the wrist. These pass under the extensor retinaculum within a common synovial sheath. The tendons end into the extensor expansions of the fingers. Tendons to the ring and the little finger often fuse. EDS is supplied by nerves C7 and C8. The EDS enables the extension of wrist and index finger, along with other fingers.

It is a well known phenomenon that EMG is a non-linear signal as is the case with most of the physiological signals. Attempts to relate the EMG with the joint variables in the presence of arbitrary movements have met with little success. EMG signal pattern depends on lot of parameters including speed of movement, amplitude of movement, load on the joint and number of muscles activated at one point of time. It also depends on the position of measuring electrodes with respect to the activated muscle. The dependence of the SEMG on these factors makes it extremely difficult to predict the joint angle of the index finger, using normal signal processing techniques. Therefore, an Artificial Neural Network (ANN), with its ability to predict the output from non-linear signals, might be a useful tool for the prediction of the joint angle of the index finger.

2.9 Neural Networks

The structure of an ANN is inspired by the organization of human brain and therefore, to understand an ANN we need to understand the basics of human brain. A human brain is a highly developed data processing module capable of analyzing a vast amount of visual, auditory and sensory information. It is superior to even the most advanced AI system based on the fastest supercomputer designed for the recognition of

objects and faces. A human brain typically consists of a very complex structure of around 100 billion neurons that are densely interconnected to 1000 to 10000 connections per neuron. The switching times of the fastest neuron in a human brain are known to be of the order of 10^{-3} seconds, and are quite slow compared to computer switching speeds of 10^{-10} seconds. Yet, humans are able to make surprisingly complex decisions, surprisingly quickly, in the order of 10^{-1} seconds. It is quite evident that the neurons firing sequence in 10^{-1} seconds cannot be more than a few hundred steps, even though the efficiency is extremely high as compared to a computer. This observation has led many to speculate that the information-processing abilities of biological neural systems must follow from highly parallel processes operating on representations, which are distributed over many neurons. This highly efficient functioning of the brain is the prime motivation for the design of a parallel processing system based on human brain (Mitchell, 1997). A neuron is a basic processing unit of brain, which animals use to detect the outside environment, the internal environment of their own bodies, to formulate behavioral responses to those signals, and to control their bodies based on the chosen responses. All neurons have a body called a Soma. The Soma contains the nucleus and all of the other organelles that are needed to keep the cell alive and functioning. Neurons also have directionality to them. On one side of the neuron are the dendrites. The dendrites serve as the input gateway to a neuron.

The dendrites are branching structures, and connect with the outputs of other neurons. They typically spread over a wide area in the immediate vicinity of the neuron. This allows the neuron to get inputs from a number of different synapses. The other end

of neuron is the 'output' end containing an axon. The axon is usually quite long compared to the rest of the neuron. Neuron activity is typically excited or inhibited through connections to other neurons. The output of the neuron is produced only when the combine input of all the dendrites is high enough to fire the neuron. The output is then channelised through the axon, which is connected to numerous dendrites of other neurons through synapses containing a neurotransmitter. Synapses usually connect to the dendrites of other neurons or are connected directly to muscles. The transmission of the signals across these synapses is electro-chemical in nature and the magnitude of the signal depends on the synaptic strength of the synaptic junction. The strength of the conductance of a synaptic junction is modified every time the brain learns. This process can be best illustrated by the example of driving on a new road. The first timer always finds it difficult to drive on a new road. On the contrary, the person who has driven on the same road for many times even remembers the potholes on the road. Human brain always associates a particular event or picture to a similar event that has happened in the past, or the picture he has seen before and passes the judgment based on the past experience.

An ANN is a highly organized structure of parallel processing units called as neurodes, the organization of which is inspired by the architecture of cerebral cortex portion of human brain. Neurodes are analogous to neurons in the brain as they have inputs (dendrites) and the output is the weighted function of the input. Neurodes are sequentially arranged in different layers with full or random connection between layers. The figure 2.3 shows a McCulloch and Pitts model (MCP) neuron in a neural network.

Mathematically, a neuron is described by the following equations (Hertz et.al., 1991)

$$u_k = \sum_{j=1}^m w_{kj} x_j$$

$$y_k = \varphi(u_k + b_k)$$

where x_1, x_2, \dots, x_m are the inputs to the neuron and w_{km} are the synaptic weights of the neuron, u_k is the weighted output of the neuron which is then given to the transfer function φ . The final output of the neuron is y_k which is obtained by adding a bias b_k to the neuron output u_k , and passed through the transfer function φ .

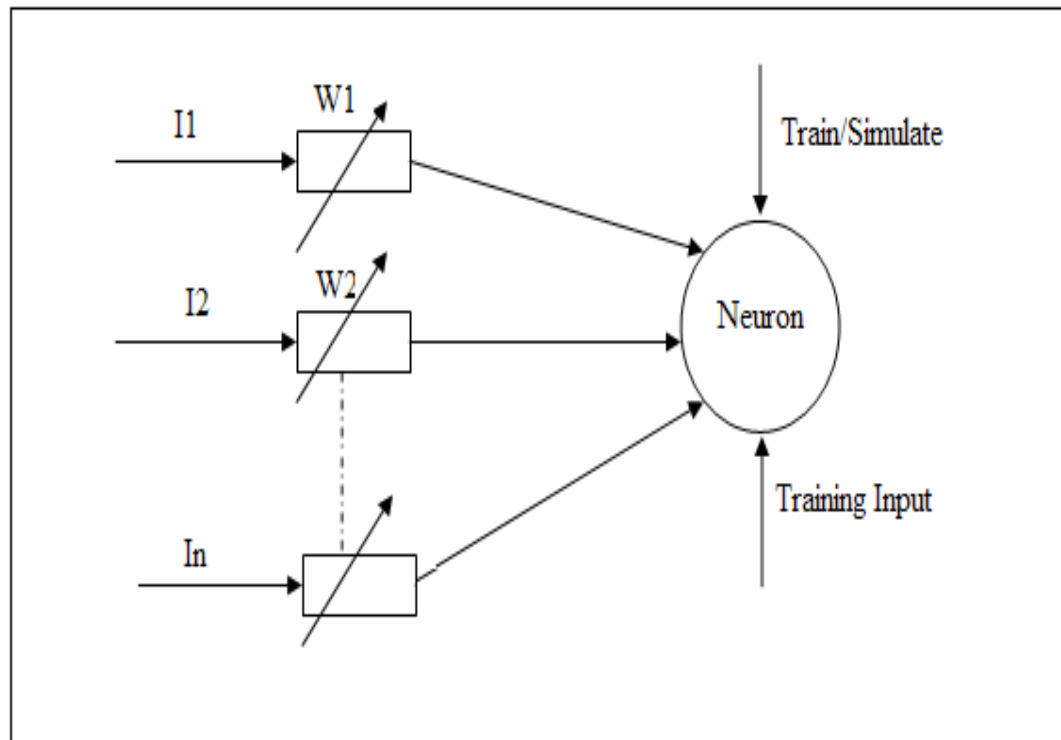


Figure 2.3 McCulloch and Pitts model (MCP) neuron. I1 through In are the inputs and W1 through Wn are the corresponding weights attached to the inputs.

A typical neural network consists of one input layer, one output layer and one or more hidden layers. Figure 2.4 shows the diagram of a typical neural network. Each neurode is unidirectional and connected to the other neurode of the next layer through synapses. This type of architecture is called as feed forward network. A fully connected network is the one in which every neurode in one layer is connected to every neurode in the subsequent layer. The output of the each neurode is the weighted function of the inputs. The output is subjected to a nonlinear transfer function which is usually a threshold function or bias, and the output is generated only when the weighted sum exceeds the bias value. The operation of a neural network involves two stages, training and recall. Training is a process by which the desired input and outputs are given to the neural network and the network adjusts the connection weights in order to give the desired output.

The learning process is governed by a learning algorithm. Recall is the process of evaluation of a neural network response to new inputs.

2.9.1 Transfer Functions

The input output function, also called as transfer function or activation function, along with the weight of each unit, greatly affects the learning process and the output of the neurode. This function typically falls into one of three categories:

- linear
- threshold
- sigmoid

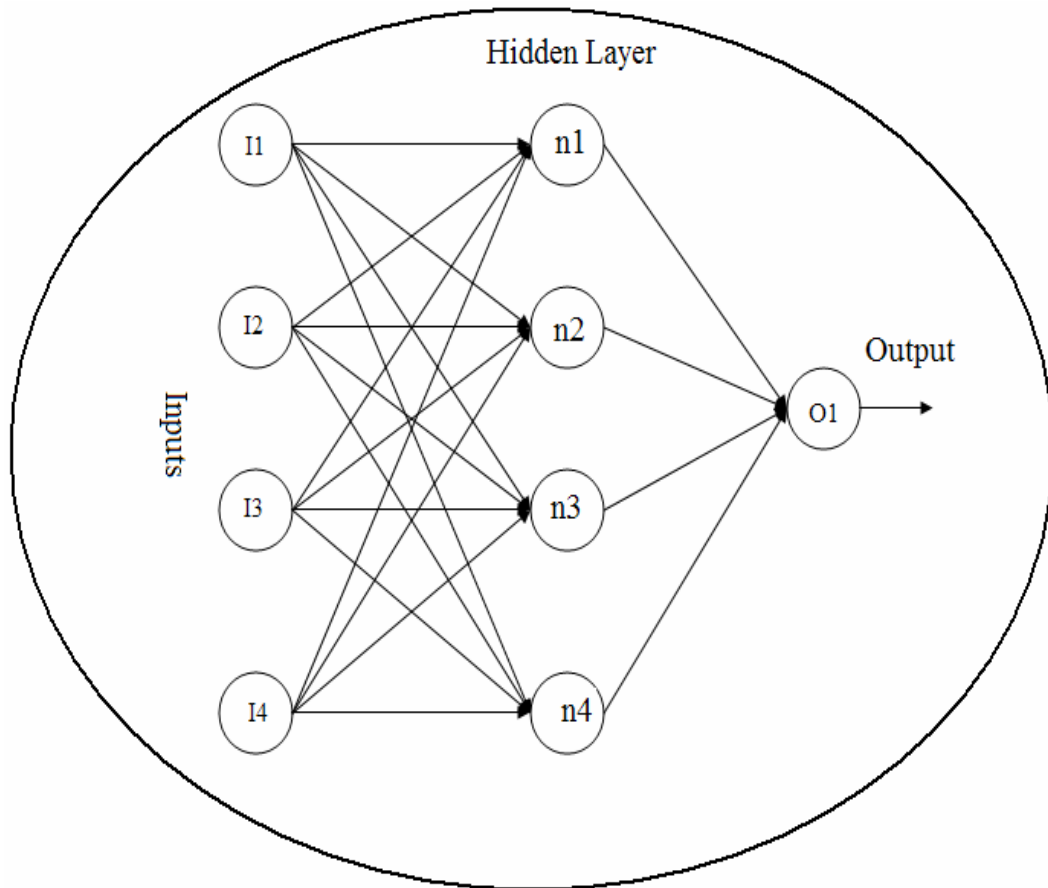


Figure 2.4 A typical two layer Neural Network

For a linear unit, the output is proportional to the total weighted input. The output value ranges from +inf. to -inf.

For a threshold unit, the output is set at one of two levels, depending on whether the total input is greater than or less than some threshold value. The output value of the neurode ranges from 1 to 0.

For a sigmoid unit, the output varies continuously, but not linearly as the input changes. A sigmoid transfer function is a smooth and continuous thresholding function of the type

$$S(x) = \frac{1}{1 + e^{-ax}}$$

Figure 2.5 shows the graphical representation of the input and output relation in a sigmoid transfer function.

For large a , the function approaches a Heaviside step function at $x = 0$. The sigmoid is frequently used as a transfer function in ANN. All the three transfer functions are rough approximations of the neurode but Sigmoid units bear a greater resemblance to real neurons than do linear or threshold units. The choice of the appropriate transfer function depends on the application of the neural networks.

2.9.2 Learning Process

The learning of the neural network is the determination of appropriate weights of neurodes for predicting the output of an unseen quantity. The learning process of a network is carried out in the following three different steps.

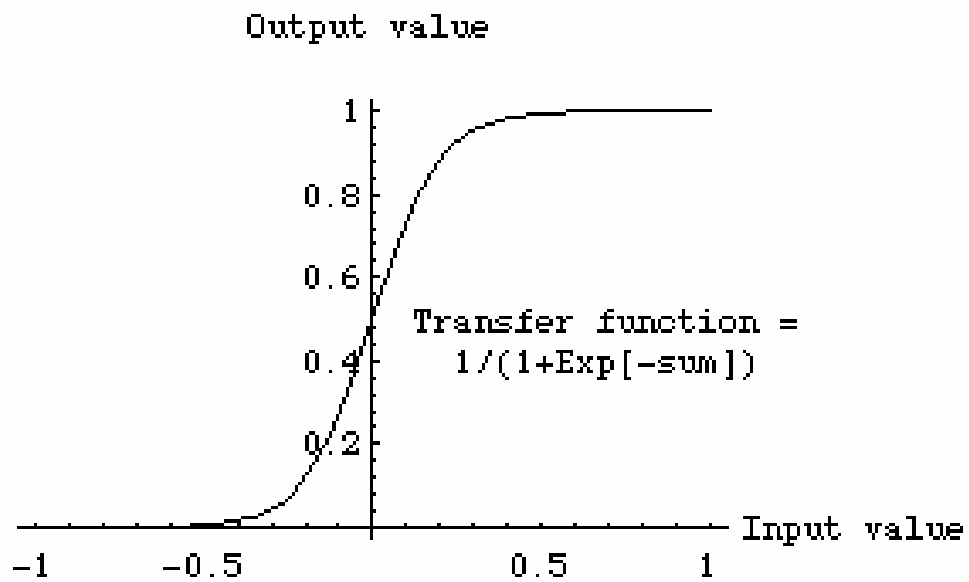


Figure 2.5 Input and output relation in a sigmoid transfer function

1. Present the network with the training examples consisting of the input pattern and the desired output for those patterns. The choice of the training data is very important for the efficient learning of a neural network. The data should cover all the pattern possibilities for the network to predict the correct output in even extreme situations. Based on the type of the data provided to the neural network, the network can be trained for either associative mapping, in which the network is trained for recognizing a particular pattern in the input data, or regularity mapping, in which the network learns to respond to the particular properties of the inputs and thereby giving a unique response of each input unit.
2. Find the error between the desired output and the output predicted by the network.
3. Change the weight of each neurode unit so that the network predicts the output with better approximations between the predicted and desired output.

The learning methods are broadly classified in two different categories.

1. Supervised learning

Supervised learning incorporates an external teacher, and each output unit is informed about the desired output for a particular input pattern. During the learning process, global information may be required. Paradigms of supervised learning include error-correction learning, reinforcement learning and stochastic learning.

2. Unsupervised learning

Unsupervised learning uses no external teacher and is based upon only local information. It is also referred to as self-organization, in the sense that it self-organizes data presented to the network and detects their emergent collective properties. Paradigms

of unsupervised learning are, Hebbian learning and competitive learning. Most of the practical problems use back propagation learning algorithms for training. Back propagation method works on error correction learning.

2.9.3 Back Propagation Learning

Back propagation learning works on the error correction method, in which the error is calculated and compared with the desired output during every iteration. The weight of each neurode is then recalculated to reduce the error, and the next iteration is performed. This process is repeated till the output error is steady. Following are the conditions in which back propagation may be a very useful algorithm.

- A large amount of input/output data is available but there is no definite relation between input and output.
- The problem appears to have overwhelming complexity however, there is clearly a solution.
- It is easy to create a number of examples of the correct behavior.
- The solution to the problem may change over time, within the bounds of the given input and output parameters.
- Outputs can be fuzzy, or non-numeric.

2.9.4 Applications of ANN

ANNs have been widely applied in the following fields:

1. Pattern recognition

2. Image processing and segmentation
3. Forecasting
4. Smart engineering systems designs

Neural networks are ideal in recognizing diseases and hence they find wide ranging applications in the field of medicine. Reddy et. al(1995) demonstrated the use of redundant neural networks and implemented them in the diagnosis of dysphagia. Salchenberger et. al (1997) used back propagation and radial basis functions for the diagnosis of breast implant rupture using ultrasound. The results showed that radial basis functions performed better in this case, as compared to back propagation techniques. At the same time Laffey (2003) used back propagation method for the prediction of residual neuromuscular block. Another application of neural networks in pattern classification is gait analysis. Su et. al (2000) used supervised feed forward back propagation neural networks for the assessment of gait patterns. Neural network can also be a very useful tool for the pattern classification of myoelectric signals (MES). Kelly et. al (1990) demonstrated the use of discrete Hopfield network for calculating the time series parameters for a moving average myoelectric signal model. They applied a second neural network for classification of a single site MES based on two parameters, time series parameter and the signal power. Abel et. al, (1996) investigated the performance of neural networks for analysis and classification of healthy subjects and patients with myopathic and neuropathic disorders, using EMG signals at maximum contraction from right biceps. Suryanarayan (1996) successfully used neural networks and fuzzy logic for the prediction of elbow joint angle using SEMG. A neural network committee can also be

employed for the task instead of a single neural network. The committee comprises neural networks which are selected from several trained neural networks with least errors. Palreddy (1993) used multiple, differently trained networks to improve the decision making process of the neural networks. Reddy and Buch (2003) used committee neural networks for speaker verifications using speech signals. Das et. al (2001) used committee neural network for the classification of normal from artifact signals for swallow acceleration. Prabhu et. al, (1994) used committee neural networks for automated recognition of acceleration signals due to dry swallowing and coughing. Shah et. al, (2005) used committee neural network for the classification of arthritis base on the finger joint acceleration signals. Researchers have shown that, with the careful selection of the training algorithm and training parameters, any non- linear signal can be classified using a committee neural network.

CHAPTER III

METHODOLOGY

The objective of the present investigation was to develop a neural network based artificial intelligent system for tracking the movement of the index finger at three different speeds. The SEMG signal was acquired from the extensor muscle (EDS) located at the posterior side of the forearm of the right hand, while the subject performed rhythmic flexion-extension rotation of the index finger at three different frequencies. A pre amplifier was specifically designed for the amplification of SEMG. The SEMG was amplified and filtered by the pre-amplifier and an instrumentation amplifier with inbuilt notch filter and band pass filter. The root mean square (RMS) of the SEMG was calculated and then was filtered using a ButterWorth low pass filter. Parameters were extracted from the RMS of the SEMG for the training of neural networks. ANNs were trained using extracted parameters as inputs, and actual angles as targets. Six types of networks were trained, which were specialized to handle the three different speeds of finger rotation. Two committees for each speed (one each for the upward and downward movement of finger) were selected for predicting the joint angle. The neural network committees were evaluated using data from subjects not used for training. The RMS errors were calculated between the actual angle and the calculated angle. These errors

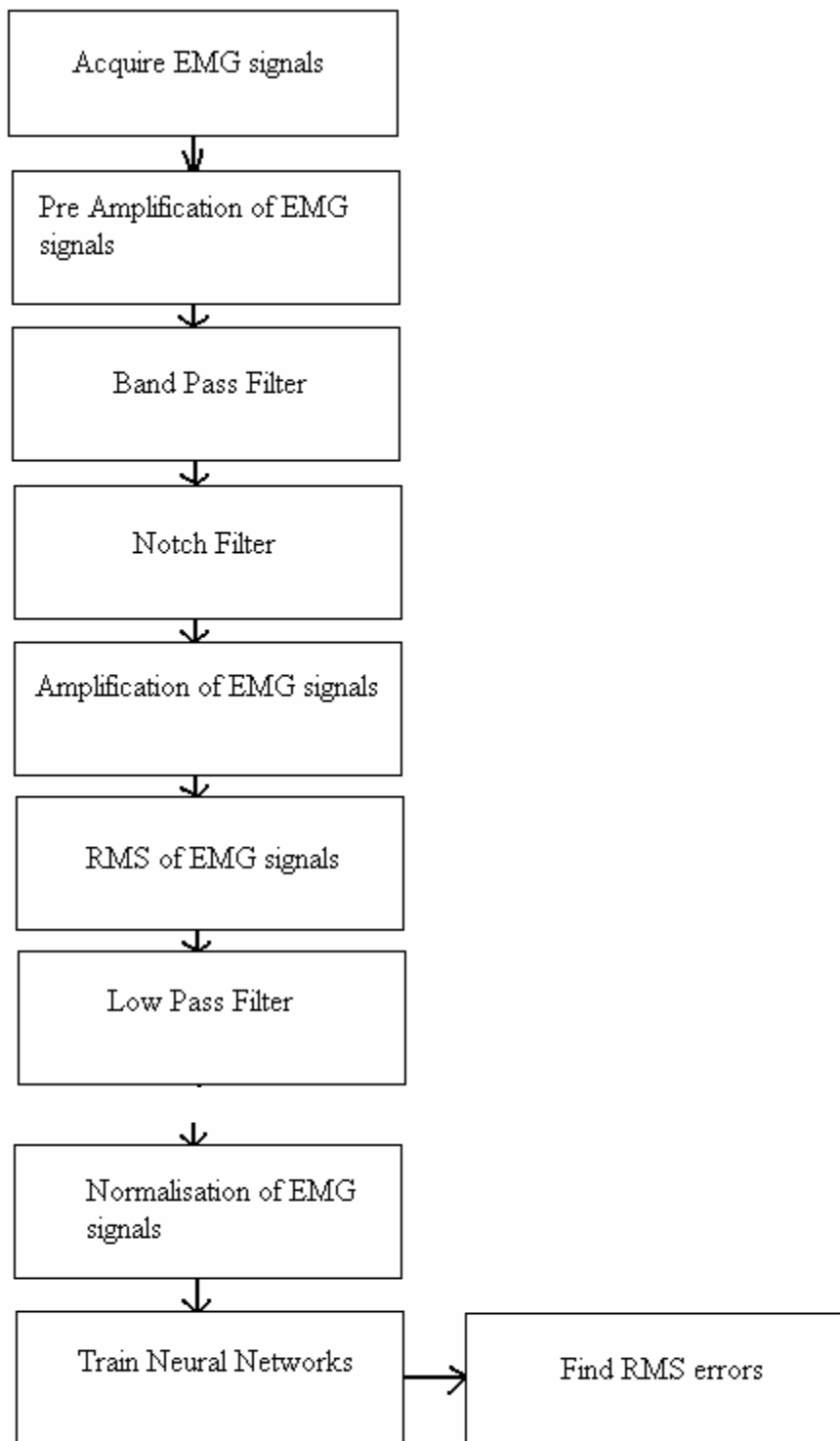


Figure 3.1: Overall Flow chart of the methodology

were used to determine the efficiency of the committee networks for predicting the angles of finger rotation. Figure 3.1 shows the overall flow chart of the project.

3.1 Instrumentation

A two stage differential pre-amplifier with a gain of 4000 was specially designed and developed to provide a milivolt output from microvolt input. Further instrumentation included an amplifier (Gould Inc, Universal amplifier, Model number 13-4615-58) with a built-in notch filter at 60 Hz and a band pass filter.

3.1.1 Differential Pre-Amplifier

The pre-amplifier designed for this project was a two stage, two channels differential pre-amplifier. The first stage was a bipolar differential precision instrumentation amplifier (INA 122) for accurate, low noise differential signal acquisition, with CMRR of 83. The gain of the first stage was 400. The amplifier operated on ± 9 volts provided by two 9 volts alkaline batteries. The output of instrumentation amplifier was DC coupled for the prevention of any DC signal passing through the circuit.

The second stage was a non inverting operational amplifier (μ A 741). The gain of the second stage was 10. The net gain of pre-amplifier was 4000. The output was provided to an isolation amplifier (ISO 124P). This stage provided protection to the subject against power line current.

3.1.2 Amplifier

Amplifier stage consisted of an instrumentation amplifier (Gould Inc, Universal amplifier, Model number 13-4615-58) with a band limit capacity from 0-10K Hz. The amplifier provided a variable gain from 0.5-240. The table 3.1 shows the technical specifications of the system. Figure 3.2 shows the block diagram of the instrumentation system.

3.2 Location and Placement of Electrodes

The SEMG signal was measured using silver/silver chloride SEMG electrodes (Myotronics-Noromed, Inc., DUO-TRODE) with an inter-spacing of 21 ± 1 mm. A pair of electrodes was attached over EDS on the posterior side of the forearm. The muscle was identified by palpation. Some of the precautions taken during the placement of electrodes include:

- Before the placement of electrodes, the skin was properly cleaned and moistened using alcohol swabs.
- The muscle was carefully palpated by asking the subject to rhythmically flex and extend the index finger. Electrodes were placed along the longitudinal midline of the muscle. The longitudinal axis of the electrode (which passes through both detection surfaces) should be aligned parallel to the length of the muscle fibers.

Table 3.1: The technical specifications of the system.

Amplification	96000
Input Impedance	50 M Ω
CMRR	85db -(100 Hz)
System Noise	<7 μ V- (RMS)
Resolution	0.5 μ V
Bandwidth	30 - 300Hz
Power Consumption	0.045 μ W

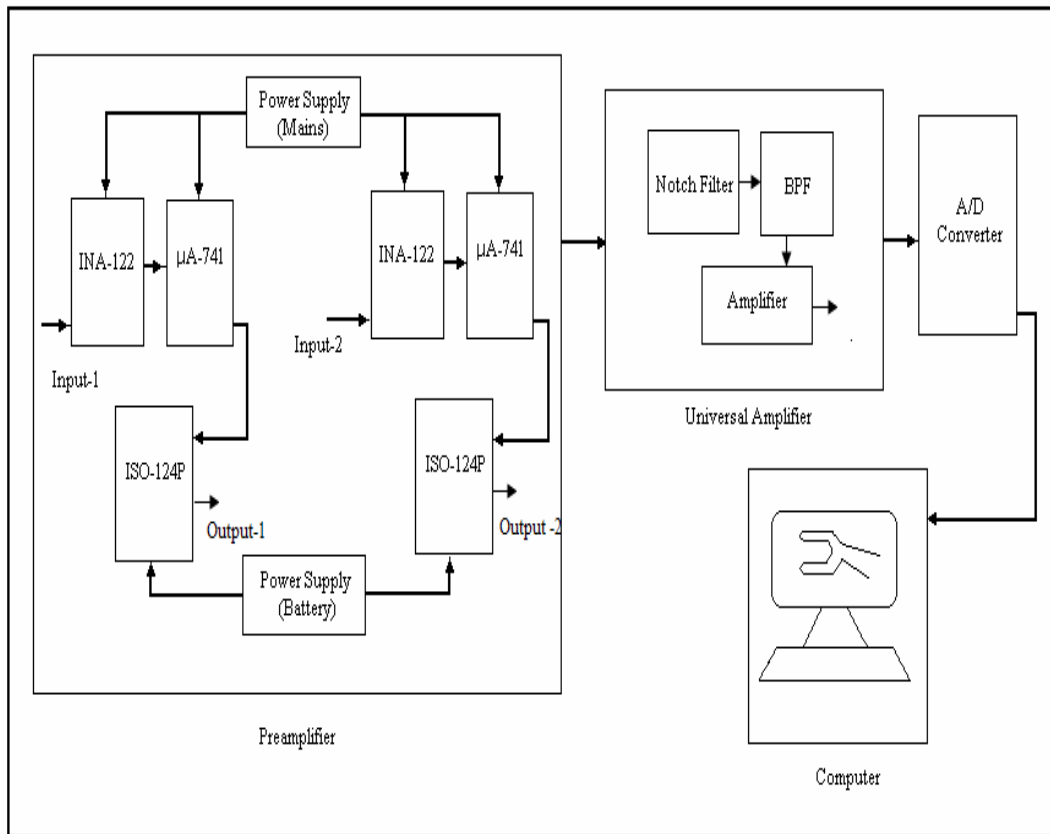


Figure 3.2: Block Diagram of the Instrumentation System

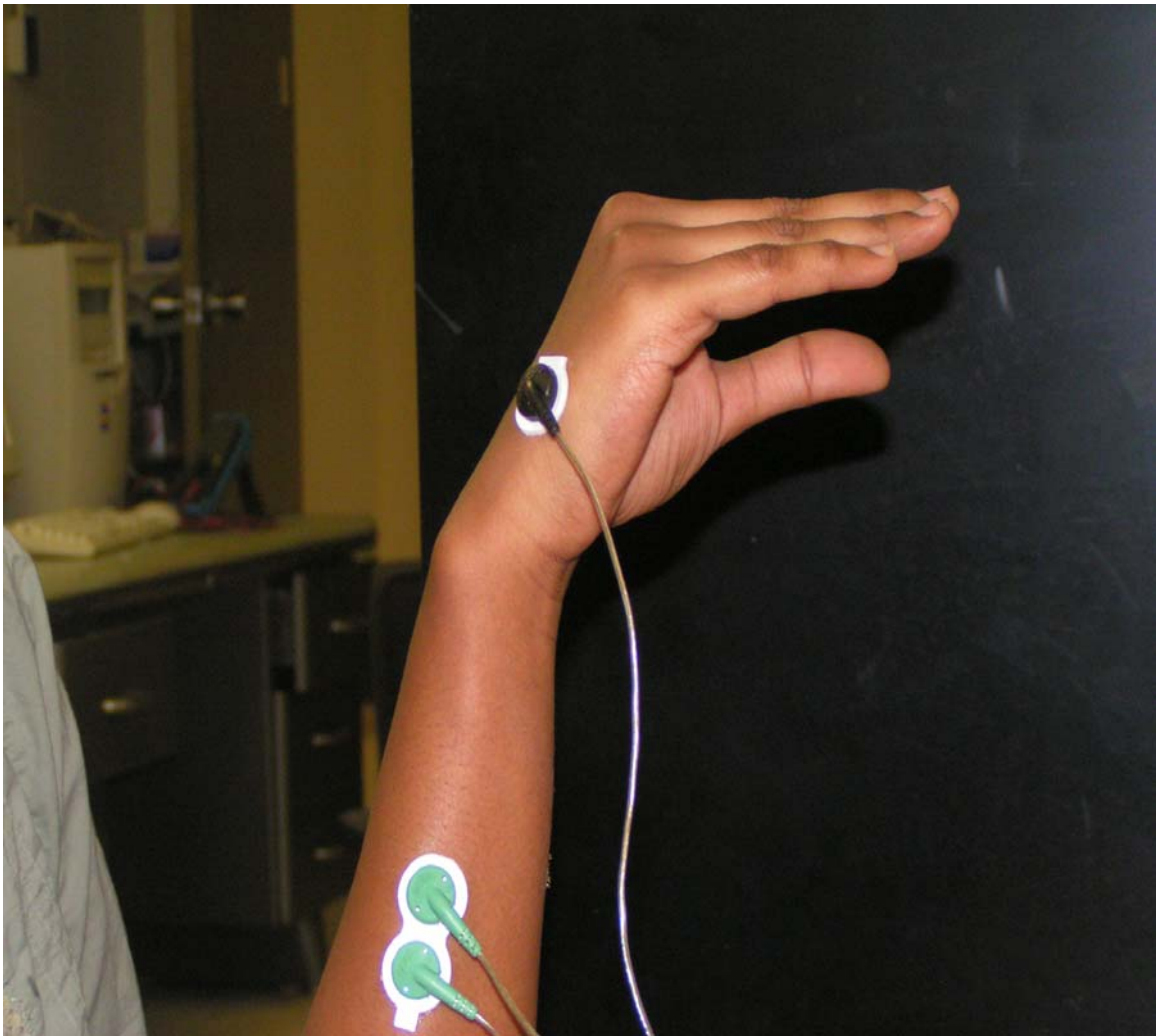


Figure 3.3: Locations and Placement of Electrodes on the Posterior Forearm of the Subject

3.2.1 Placement of reference electrodes

It is necessary that the reference electrode is as far as possible from the active electrodes and does not interfere with the SEMG acquired from the active electrode. The reference electrode was placed on the bony surface of the metacarpal near little finger. Figure 3.3 shows the placement of electrodes on the forearm of the subject.

3.3 Choice of Subjects

Subjects without any known history of any neuromuscular disorder were chosen for the study. The subjects were within the age group of 20-28 years. The study was approved by the Institutional Review Board (IRB) at The University of Akron. Participation of the subject was completely voluntary. The subjects were verbally explained the purpose and the procedure of the study, and were asked to sign a consent form (A-2). The subjects were free to withdraw from the study at any point of the time during the study.

In total, 15 subjects were used for the study. Six subjects were used to train the neural networks. Two subjects were used for initial testing of neural networks. Further, the neural networks were evaluated using 7 different subjects.

3.4 Protocol

The subject was asked to rest the right arm on the table with forearm in vertical direction and the wrist and phalangeal joints folded, and index finger in horizontal direction. An ultra miniature accelerometer was taped on the index finger of the subject at

two inches from the metacarpophalangeal joint of the index finger. The EDS was identified on the posterior forearm of the subject by palpation. The skin was moistened using an alcohol swab. A pair of SEMG electrodes was attached to the skin over the muscle such that the longitudinal axes of the electrodes were parallel to the longitudinal axis of the muscle. The subject was asked to rest the thumb on a platform raised on the stand. The height of the platform was adjustable and it was adjusted according to the comfort of the subject. This arrangement ensured that the thumb of the subject did not move. Also, the arrangement reduced the strain on the muscle during measurements.

Two sets of data were recorded. The first set of the data was used for calibration of the system and normalization of the data. The second set of data was used for prediction of the joint angle. During the data acquisition for the calibration, the subject was initially asked to relax the muscle. Then, the subject was asked to move index finger at three different constant speeds from full flexion to full extension without applying any force (figure 3.4-3.5). The speeds used for the calibration were 0.4 Hz, 0.8 Hz and 1.2Hz. The speed of the movement was controlled by an audio feedback generated by a beep sound. The subject was asked to complete one cycle in between two beep sounds. The SEMG was recorded for approximately 20 seconds for each speed. Maximum and minimum SEMG of the subject was calculated, which was later used for the normalization of the SEMG during angle prediction. In the second set, SEMG and accelerometer data was recorded after the subject was fully relaxed after the first set of data. There was no change in the settings during the first and second set of data acquisition. The subject was asked not to move other fingers and wrist during the

acquisition of data for each set. The second set of data was also recorded for three different speeds, 0.4 Hz, 0.8 Hz and 1.2 Hz.

3.5 Data Acquisition

The SEMG signal from the surface electrodes was fed to a differential two stage preamplifier with the first stage gain of 400 and second stage gain of 10. The signal was filtered and amplified in the instrumentation amplifier (Gould Inc, Universal amplifier, Model number 13-4615-58). The signal was band limited from 30 Hz to 300 Hz. The signal was notch filtered by an inbuilt notch filter and amplified by a factor of 24. Thus, the overall gain of the system was 96000.

The amplified signal was digitized at a sampling rate of 1 KHz using a 12 bit A/D converter (Dataq, WINDAQ, DI 200) and acquired onto a PC using data acquisition software (WindaqPro) . The data acquisition interface used by WINDAQ was DI-205. The resolution of the WINDAQ system was 0.0048 V. Signal from the accelerometer was directly fed to the A/D converter and sampled at a rate of 1 KHz.

3.6 Signal Processing

The signals acquired from the A/D converter were subjected to further processing.

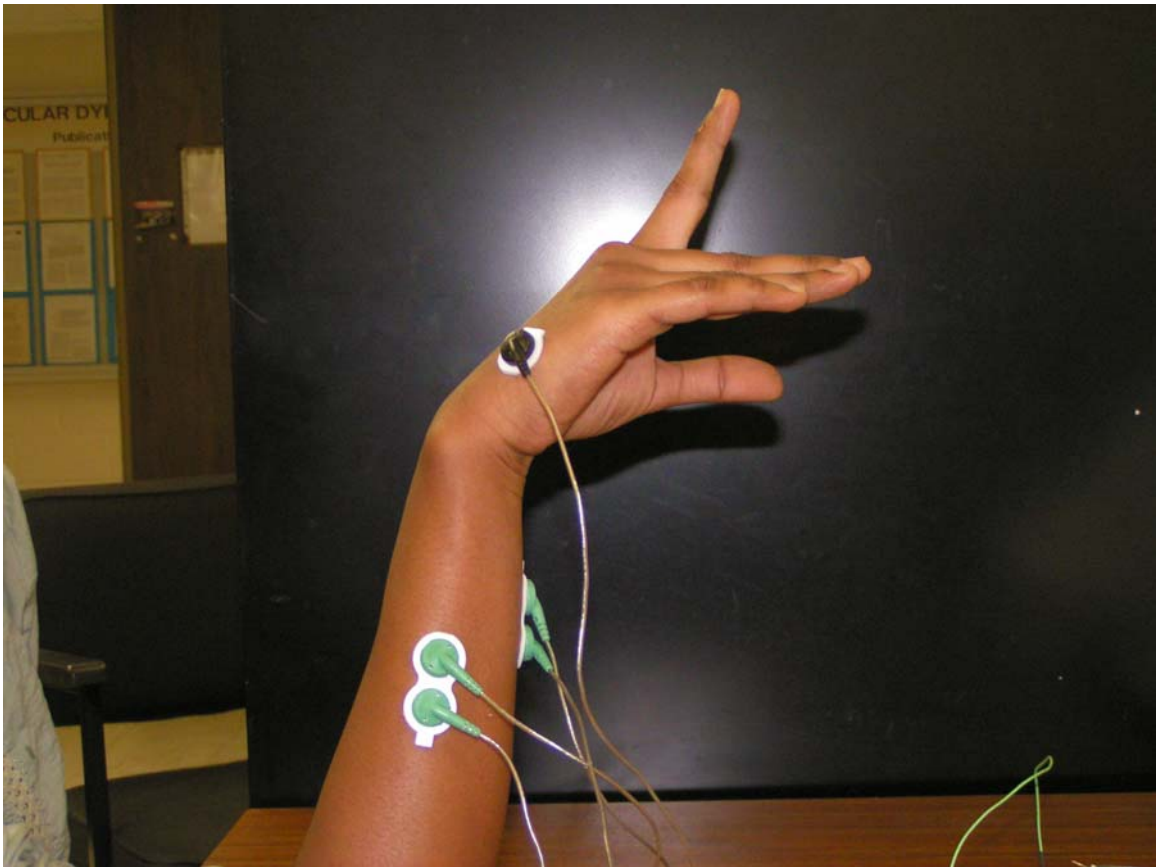


Figure 3.4: The full extension position of the index finger.

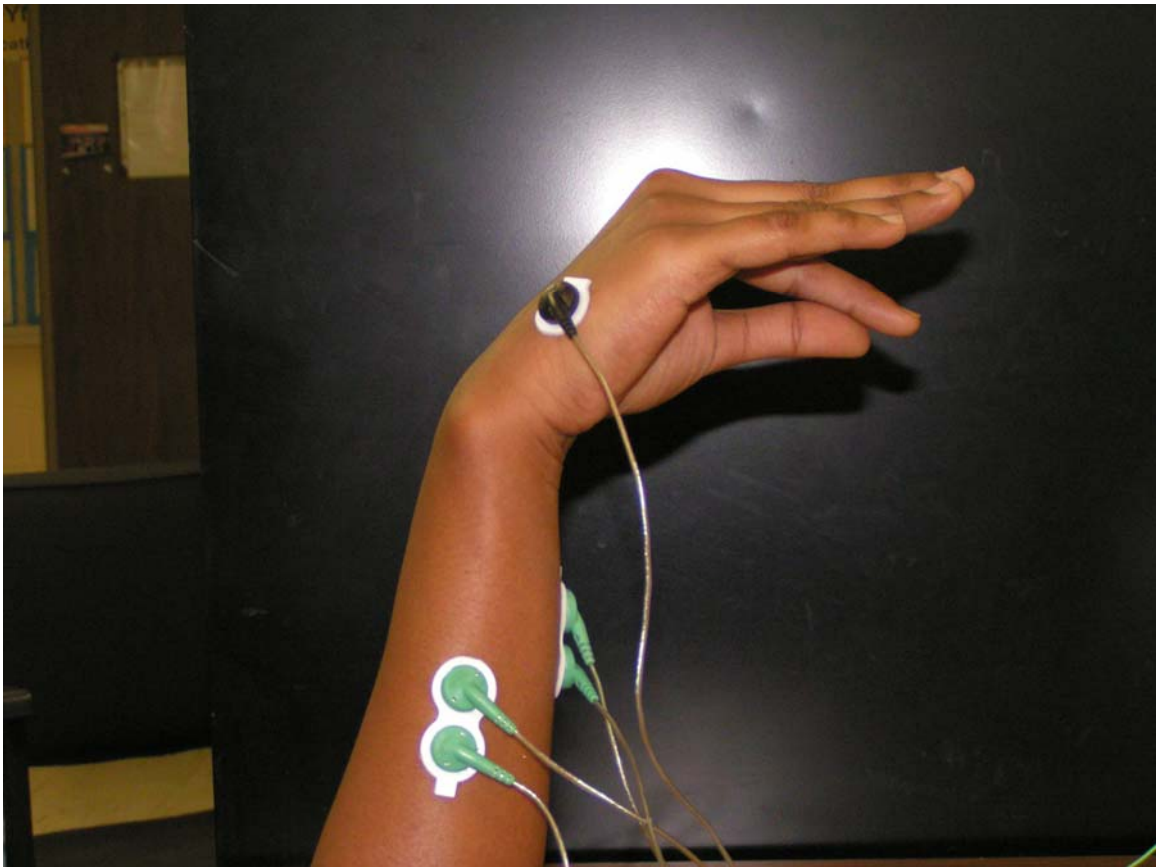


Figure 3.5: The full flexion position of the index finger.

3.6.1 Processing of SEMG signals

3.6.1.1 RMS EMG

A 10 data point moving window RMS of the digitized signal was obtained using the equation given below.

$$\text{RMSEMG}(n) = \sqrt{\frac{1}{N} \sum_{k=1}^N x(n-k)^2}$$

Where:

x = SEMG measured

N = number of data points of SEMG used

n = present SEMG data point.

3.6.1.2 Filtration

The RMS signal was then low pass filtered using a second order digital ButterWorth low pass filter at a cutoff frequency of two Hz. The equation of the filter is given as (Pashtoon, 1987)

$$H(z) = \frac{(1 + Z^{-1})^2}{(1 + a * Z^{-1} + b * Z^{-2})}$$

Where:

a, b are coefficients of the filter.

3.6.1.3 Calibration calculations

The system was calibrated for each subject. The subject was asked to move the finger at all the three speeds. The RMS of the SEMG was calculated and the RMS was

filtered using the filter described above. This data set was used to find the maximum and minimum values of SEMG. These values were used for the normalization of the data recorded for actual calculations.

3.6.1.4 Normalization of the signal

Maximum and minimum values of SEMG were used for the normalization of the SEMG during actual calculations of the joint angle.

$$\text{Normalized SEMG (NRMS)} = \frac{\text{SEMG}(i) - \text{MinimumSEMG}}{\text{MaximumSEMG} - \text{MinimumSEMG}}$$

Where:

SEMG (i) = filtered SEMG

MaximumSEMG = Maximum SEMG acquired during calibration

MinimumSEMG = Minimum SEMG acquired during calibration

Figure 3.6 shows the block diagram for the data acquisition.

3.6.2 Parameters Extraction

Several parameters from the NRMS of the signal were extracted to be fed to the neural networks. The different parameters extracted were:

1. Present value of the signal, NRMS (i)
2. Immediate past NRMS (i-1) value (PRMS).
3. Distant past NRMS (i-4)
4. Slope of the NRMS (i – (i-1))
5. Five points moving average of the slope of the NRMS signal , where every point represents the average of last 5 points of the slope of the NRMS signal

6. Square of the magnitude of the NRMS ($i*i$).

These parameters were given as inputs to the neural network. The output of the neural network was the joint angle. During training, the desired output was the actual angle measured by the accelerometer.

3.7 Processing of Accelerometer Data

The output data from the miniature accelerometer was subjected to a 10 point moving average window.

$$\text{Avgaccel}(i) = \frac{1}{N} \sum_{k=1}^{10} \text{Accelerometer}(i - k)$$

Where:

Avgaccel(i) = present averaged value of the accelerometer data.

Accelerometer ($i - k$) = past 10 values of the accelerometer.

$N = 10$, length of the moving window.

The accelerometer data was then low pass filtered by a 2nd order ButterWorth filter (Pashtoon, 1987). Several trials were performed to determine the appropriate cut off frequency for the low pass filter between 1 to 10 Hz. Preliminary results showed that the best results could be achieved for the cut off frequency of 2 Hz and hence 2 Hz was chosen as the cut off frequency.

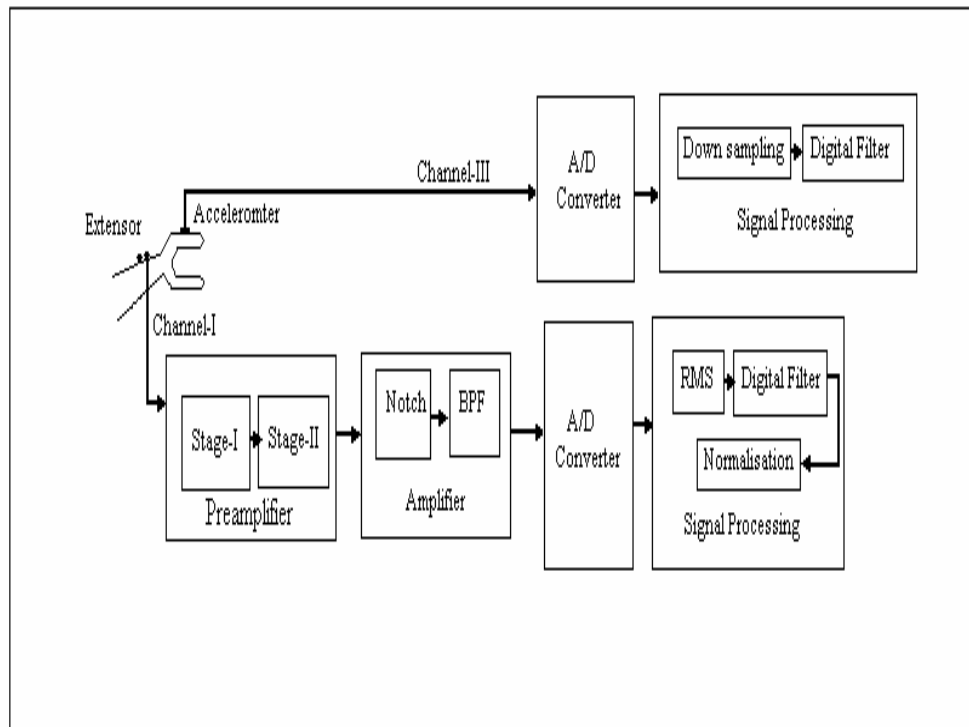


Figure 3.6: Block diagram of the data acquisition system.

3.7.1 Determination of the angle from accelerometer voltages

The corresponding angle from the accelerometer voltage was determined on the basis of the accelerometer calibration data. These angle values were used as the target parameter for the training of the neural networks.

3.7.2 Accelerometer Calibration

A miniature single axis- accelerometer was used for the measurement of the actual joint angle of the movement of the index finger. The output of the neural network was compared to the output of the accelerometer for calculation of the RMS errors. The accelerometer was a gravity based tilt sensor. The specifications of the accelerometer are tabulated in table 3.2. The output of the accelerometer was voltage and therefore, it was calibrated for the corresponding angle of rotation.

For calibration, the accelerometer was mounted on the protractor, on a movable platform. The height of the platform was adjustable, representing the actual measurement conditions. Following steps were performed for the calibration of accelerometer.

1. The accelerometer was fixed on the horizontal aluminum plate, parallel to the arm of the protractor.
2. The protractor arm was moved every five degrees and the output voltage of the accelerometer was recorded using WINDAQ data acquisition system.
3. Six datasets were acquired using the same step as step two, and the average measurement at every five degrees was used for the calculation of corresponding angle.

4. Voltage change per degree was calculated for every five degrees and the corresponding voltage for every degree of angle was calculated.
5. Step two and step three were repeated for different positions of the accelerometer on the aluminum arm.
6. Step two and step three were repeated for different heights of the adjustable stand.
7. The range of measurement was -40 degrees to 60 degrees with zero degrees as the neutral position.

Measured angle was plotted against the measured voltage and a regression analysis was performed. The linearity for the accelerometer angle Vs accelerometer voltage was found to be 0.9988. Figure 3.7 shows the plot of Accelerometer Voltage Vs Angles.

3.8 Development and Training of Neural Network

The development of the neural network was a very important step in the prediction of the joint angle. Following were the steps followed for the development of the neural networks.

1. Training of the neural network.

The neural networks were trained by the six parameters extracted from the SEMG.

The data was divided in six different groups

- Slow up

This group included the data from subjects when they were moving the index finger from flexion region to the extension region at 0.4 Hz.

Table 3.2: The technical specifications of the accelerometer

Length	5mm x 5mm x 2mm
Resolution	1mg-(60Hz)
Sensitivity	1000mV/g
Bandwidth	10Hz
Operating Range	3-6V
Power	700 μ V-(Vs = 5V)
Temperature Range	-40°C to 125°C

- Slow down

This group included the data from subjects when they were moving the index finger from extension region to the flexion region at 0.4 Hz.

- Medium up

This group included the data from subjects when they were moving index finger from flexion to extension region at 0.8 Hz.

- Medium down

This group included the data from subjects when they were moving the index finger from extension to the flexion region at 0.8 Hz.

- Fast up

This group included the data from subjects when they were moving the index finger from flexion to extension region at 1.2 Hz.

- Fast down

This group included the data from subjects when they were moving the index finger from extension to flexion region at 1.2 Hz.

Data from six different subjects were used for the training of the neural networks. Training was performed using MATLAB (MathWorks). 20 neural networks were trained for each group, with extracted parameters as inputs and output angles from accelerometer data as targets. Several different training algorithms were tried before deciding on 'trainrp'. The parameters that influenced the decision included convergence and speed of the convergence. The up data were separated from down data by the slope of NRMS. Up data had positive slope while the down data had negative slope. The networks were

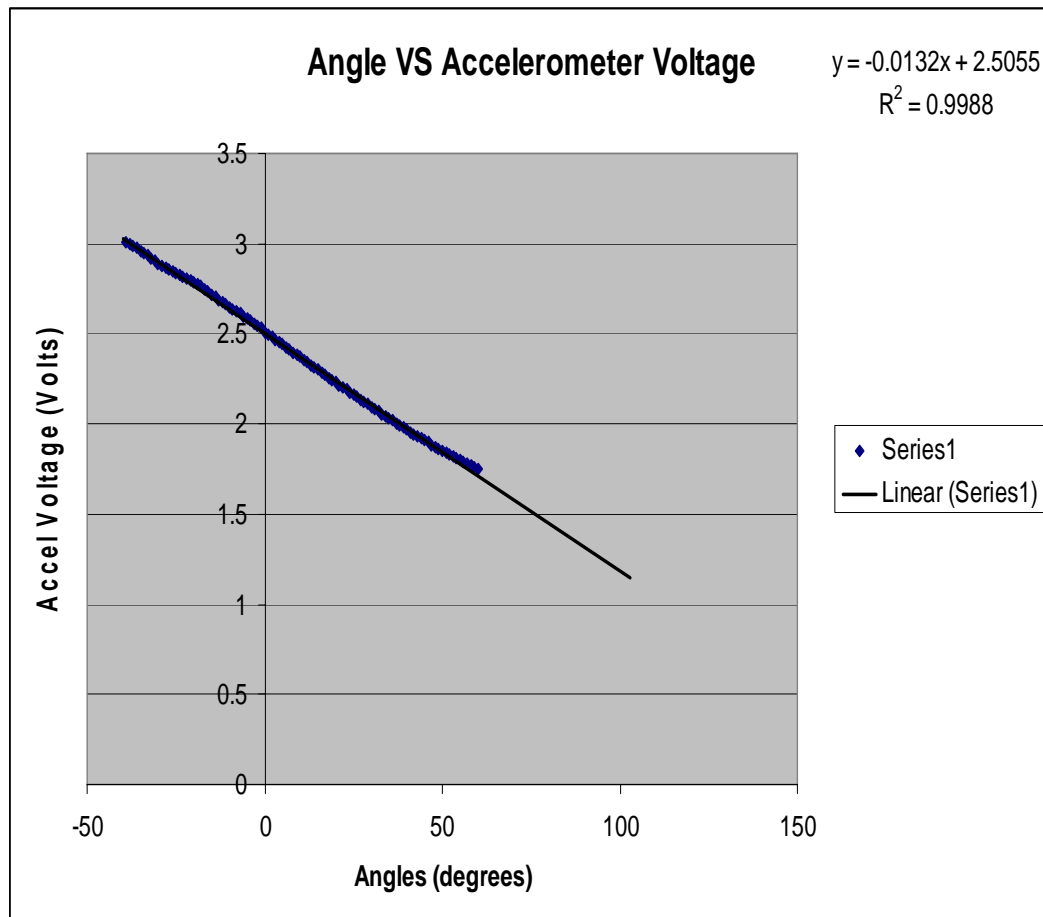


Figure.3.7: Plot of the Voltage output of the accelerometer and the angle.

trained with different number of hidden layers (1-2), different initial weights, and different number of neurons in the hidden layer (5-15). Different activation functions (tansig, logsig) were tried for the training of the networks.

2. Committee recruitment

Each network was subjected to initial testing for its performance. Data from two new subjects was used for the initial evaluation of the networks. The results of the evaluations were used for the selection of best five networks from each group for their inclusion in the respective committees.

In all, six committees, one for each data group, were formed based on the performance of the networks using data from the two new subjects.

3. Final Evaluation of the datasets

Data from nine subjects was used for the final evaluation of the committee. The respective committee for each group was subjected to the data from each individual subject. The output of the committee was the average of all the networks in the committee. Two outliers were first eliminated and the final output was the average output of the remaining networks. The final output was compared with the actual angle measured by accelerometer output.

3.9 Analysis of the results

The output angles predicted by the committee neural networks were compared with the actual angles measured by the accelerometer. RMS errors were calculated between the measured and the predicted angle.

CHAPTER IV

RESULTS

The present study demonstrated the use of the SEMG from extensor muscle for the prediction of joint angle of the movement of index finger at three different speeds. The SEMG signal along with joint angle was successfully obtained from 15 normal subjects during dynamic flexion and extension rotation at three different frequencies. Six committees of neural networks were trained and recruited to predict index finger angle using parameters extracted from NRMS. Committee evaluation showed RMS errors in the range of 3% - 25% (Table 4.1).

4.1 Results from Data Acquisition

Each subject was asked to perform rhythmic flexion and extension of the index finger with thumb, wrist and all other fingers stationary, at three different speeds of 0.4 Hz, 0.8 Hz and 1.2 Hz. Figures 4.1, 4.2 and 4.3 show the raw SEMG at 0.4 Hz, 0.8 Hz and 1.2 Hz respectively.

The figure 4.4 shows the filtered RMS EMG and figure 4.5 shows corresponding accelerometer outputs when the finger was rotated at 0.4 Hz. Similarly, figure 4.9, 4.10, 4.14, and 4.15 show RMS EMG and corresponding accelerometer output for 0.8 Hz and 1.2 Hz. The RMS EMG was normalized by maximum and minimum SEMG

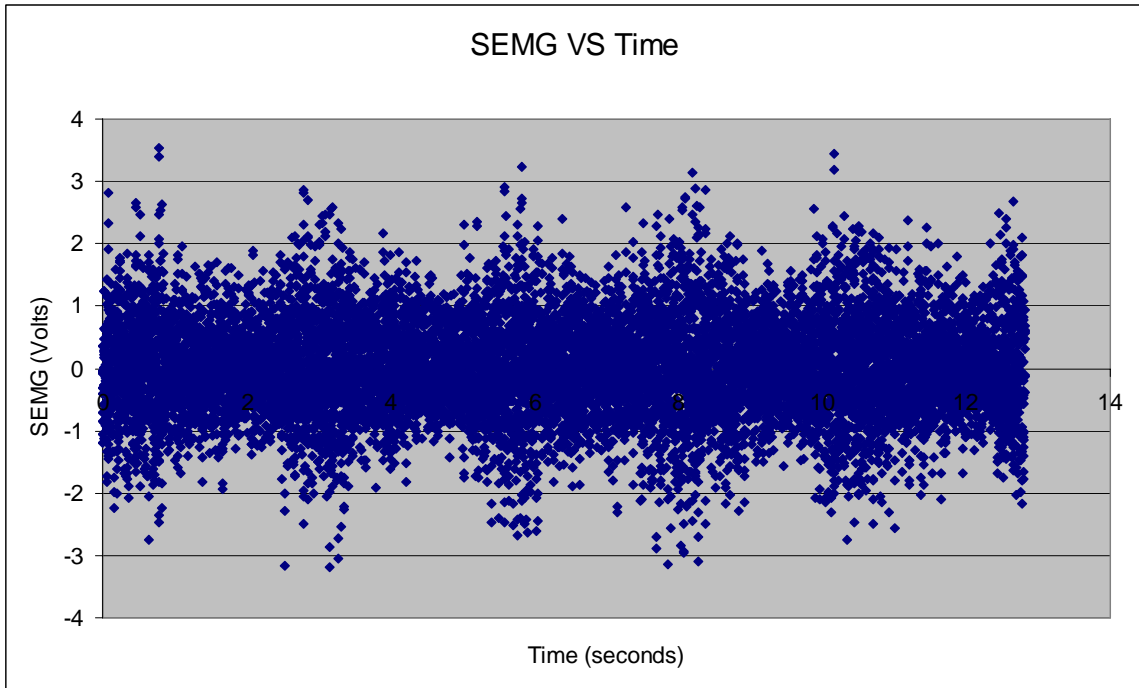


Figure 4.1: Raw SEMG acquired from EDS when the subject was performing rhythmic flexion and extension of index finger at 0.4 Hz

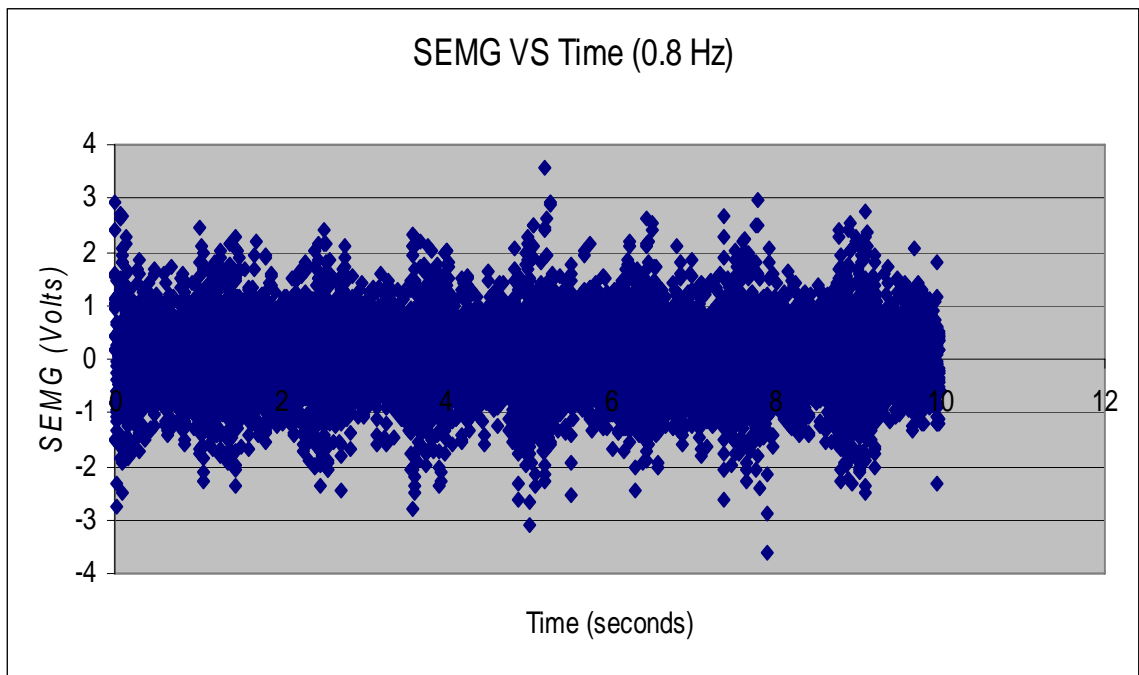


Figure 4.2: Raw SEMG acquired from EDS when the subject was performing rhythmic flexion and extension of the index finger at 0.8

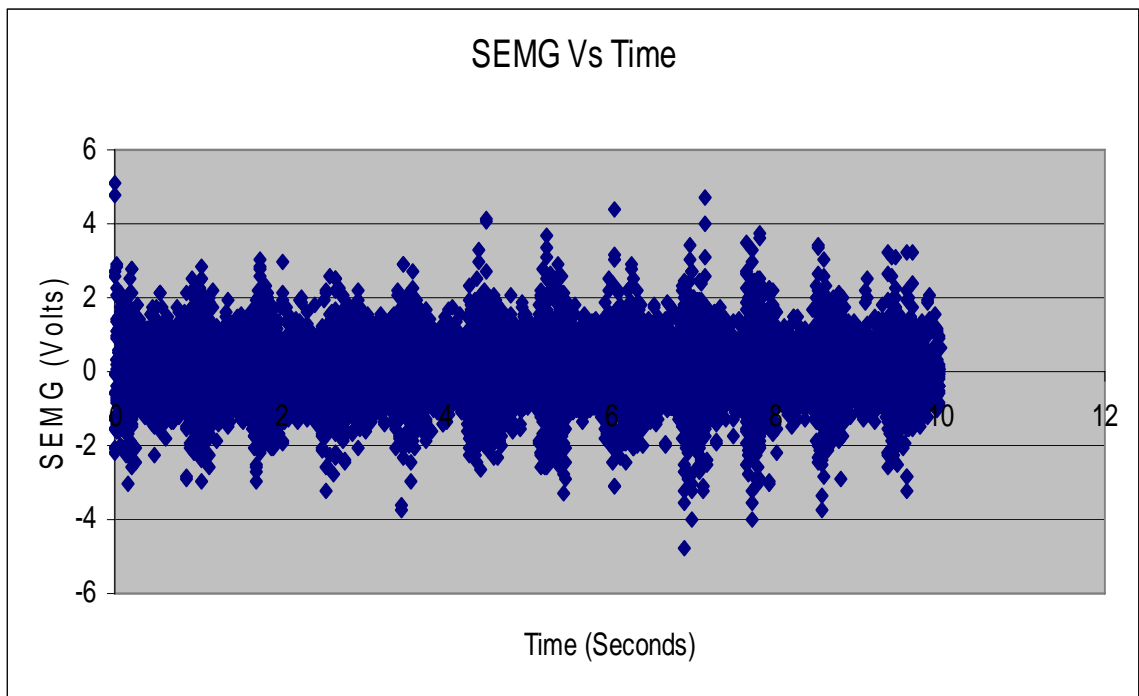


Figure 4.3: Raw SEMG acquired from EDS when the subject is performing rhythmic flexion and extension of index finger at 1.2 Hz

measured during the calibration, when the subject was asked to perform flexion and extension of index finger at all the speeds. Accelerometer output was converted to the corresponding angle. This angle was then normalized by dividing with 90 degrees, which corresponded to the maximum range of rotation (-30-60 degrees). The figures 4.6, 4.11 and 4.16 show the plot of actual angles as measured by accelerometer for 0.4 Hz, 0.8 Hz and 1.2 Hz respectively. Figures 4.7, 4.12 and 4.17 show the plot of normalized SEMG and angles plotted simultaneously as a function of time for 0.4 Hz, 0.8 Hz and 1.2 Hz respectively. The plots clearly show that the SEMG leads over the angle for all the speeds. Synchronization can be achieved between the SEMG and the angles if SEMG is delayed by 0.2 seconds. The figures 4.8, 4.13 and 4.18 show the plots of normalized SEMG plotted over the normalized angle when the SEMG was shifted by 0.2 seconds. Figure 4.19, 4.20 and 4.21 show the plot of NRMS plotted against normalized angles for 0.4 Hz, 0.8 Hz and 1.2 Hz. The plots of NRMS Vs normalized angles show hysteresis for all the speeds. This trend prompted the use of different neural networks for up and down movement of finger.

4.2 Results from CNN

The filtered SEMG along with the extracted parameters were fed to the committee neural networks, trained for predicting the angle at different speeds. The plots 4.22, 4.23 and 4.24 show the predicted angles with respect to the actual angles for one cycle of rotation for 0.4 Hz , 0.8 Hz and 1.2 Hz respectively. These graphs are plotted against SEMG. It can be seen that the SEMG leads over both the actual angle as

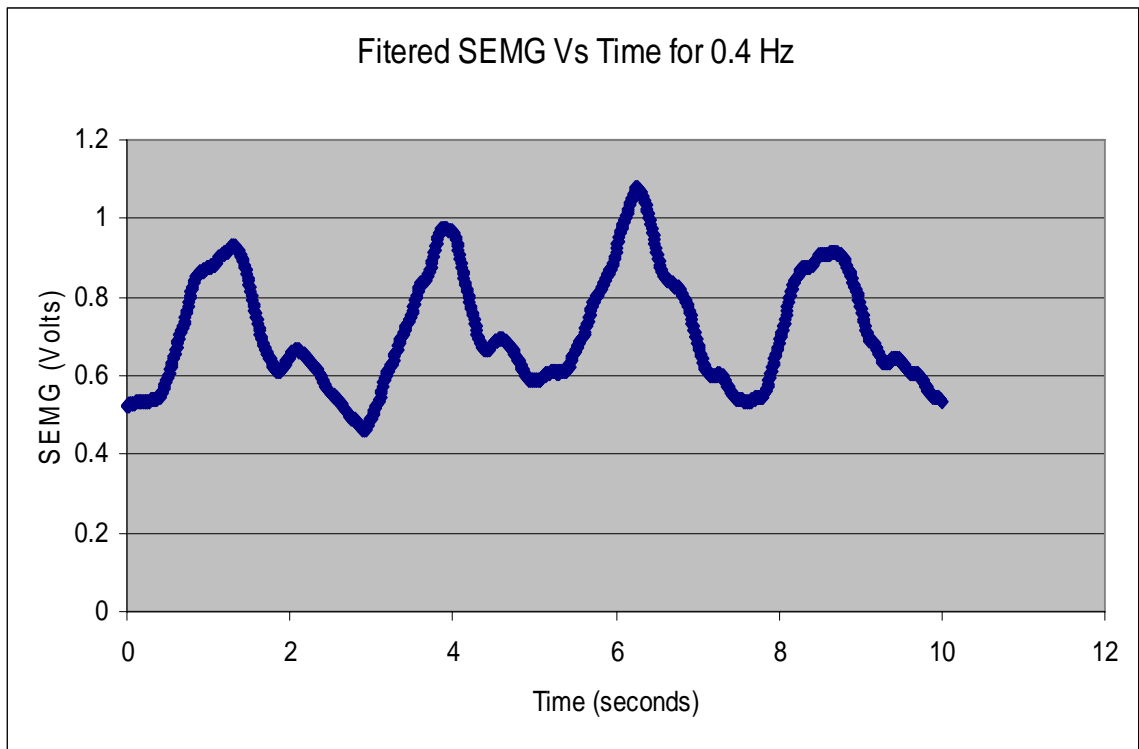


Figure 4.4: Plot of RMS SEMG Vs time for 0.4 Hz. The raw SEMG was subjected to RMS window of length 10 and was filtered with 2 Hz ButterWorth filter.

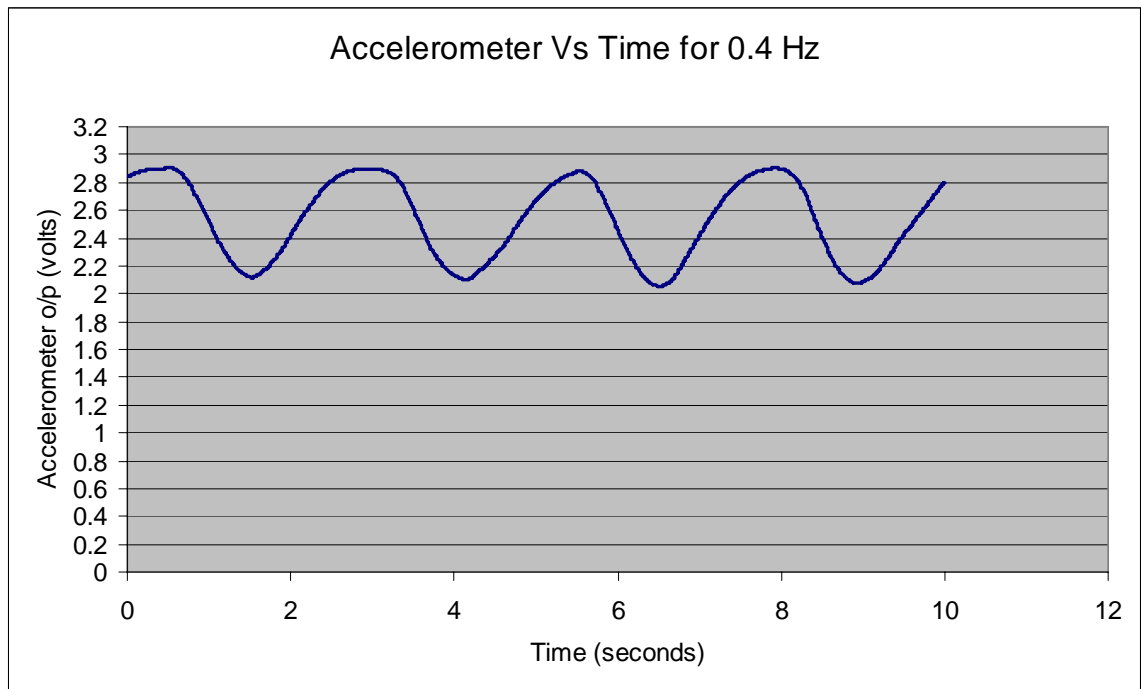


Figure 4.5: Plot of Accelerometer values plotted against time. The accelerometer was mounted on the proximal metacarpophalyngeal joint of the index finger. The accelerometer values increases as finger moves from extensor to flexor.

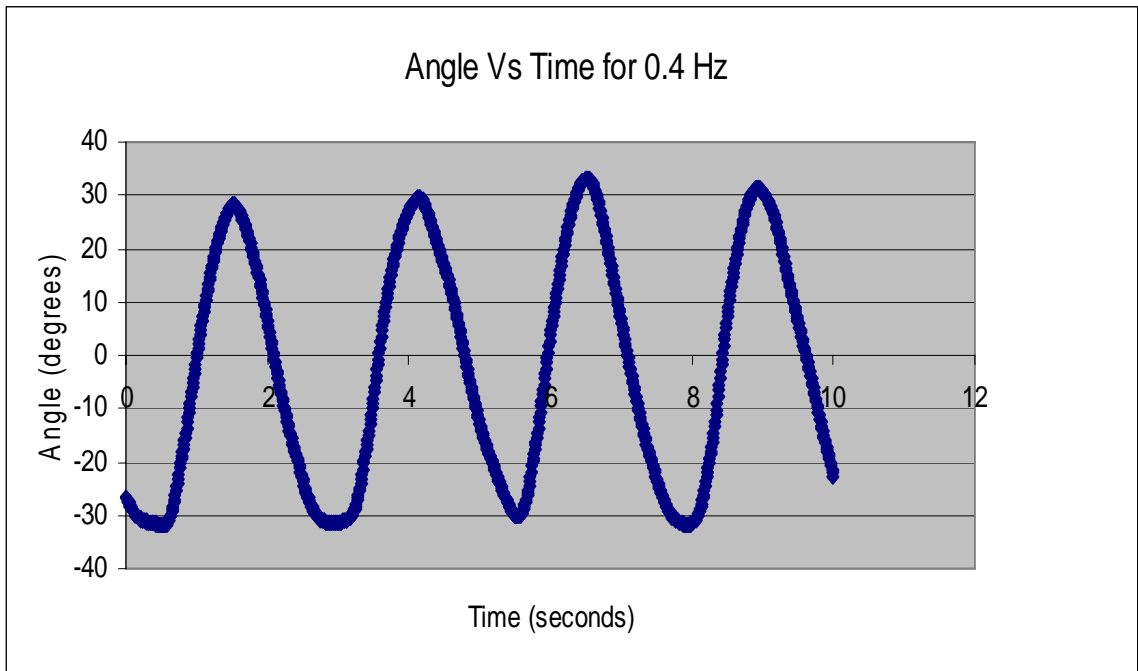


Figure 4.6: Corresponding plot of angles calculated from accelerometer values.

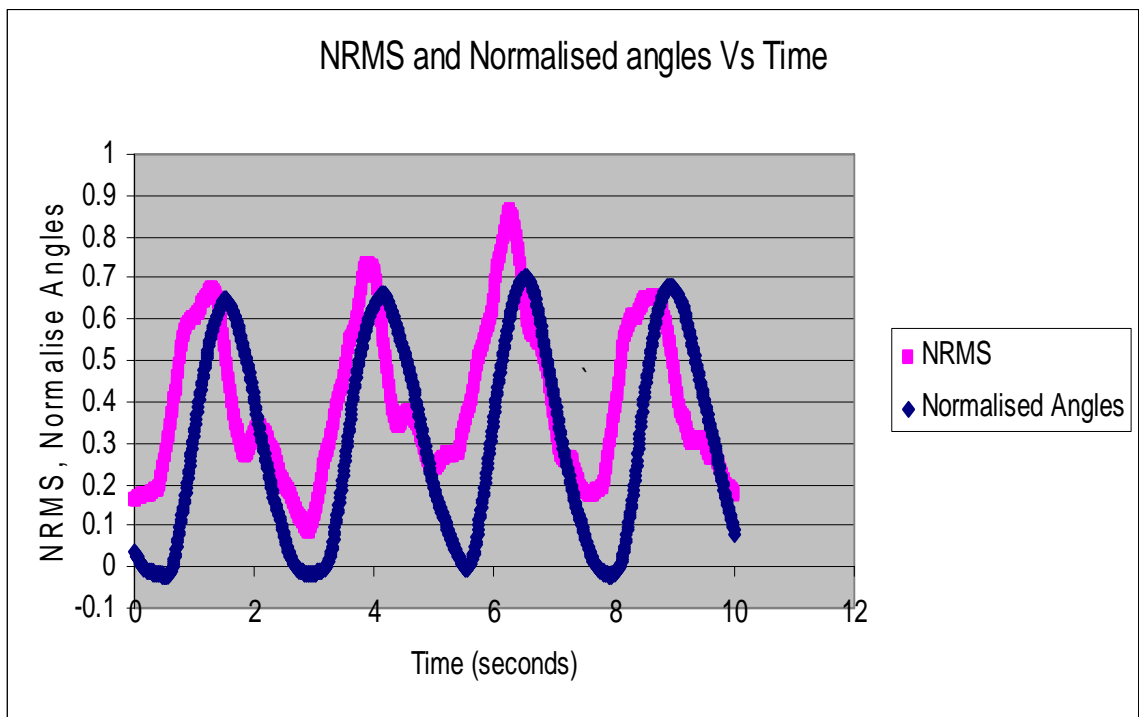


Figure 4.7: Plot of Normalized SEMG and Normalized angles plotted against time when the subject was rotating the finger at 0.4 Hz. The SEMG leads the angle plot by 0.2 seconds.

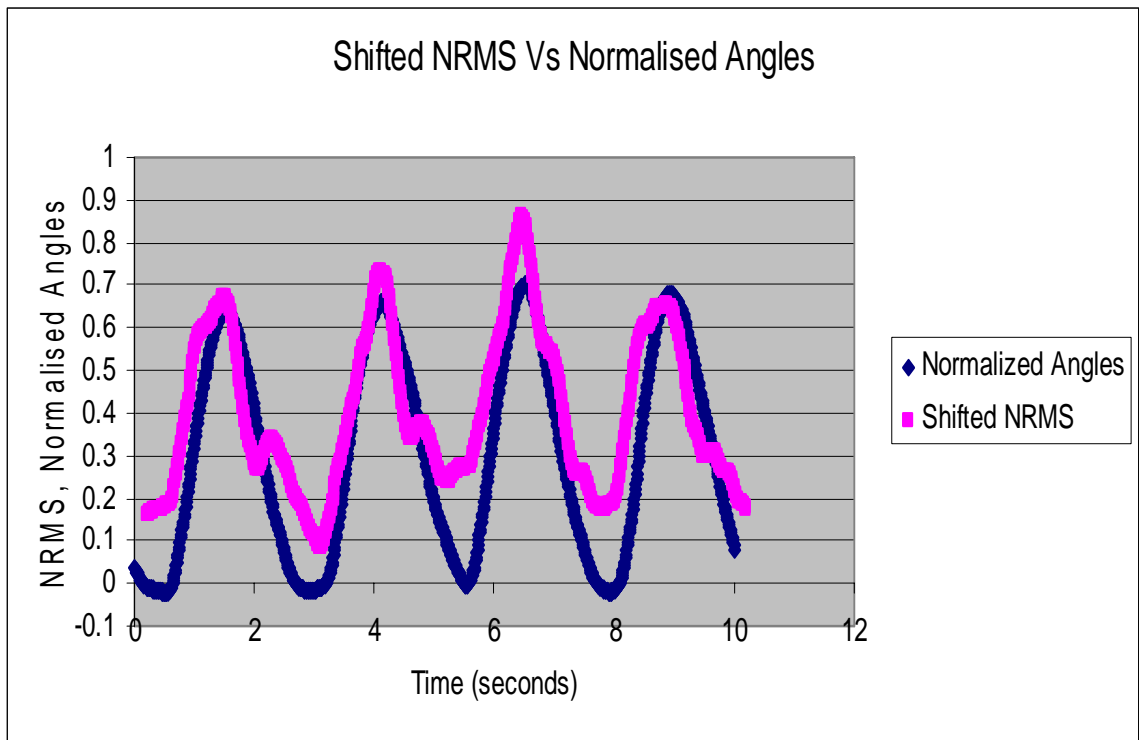


Figure 4.8: Plot of shifted NRMS and Normalized angles against time when the subject performed rhythmic flexion and extension of index at 0.4 Hz.

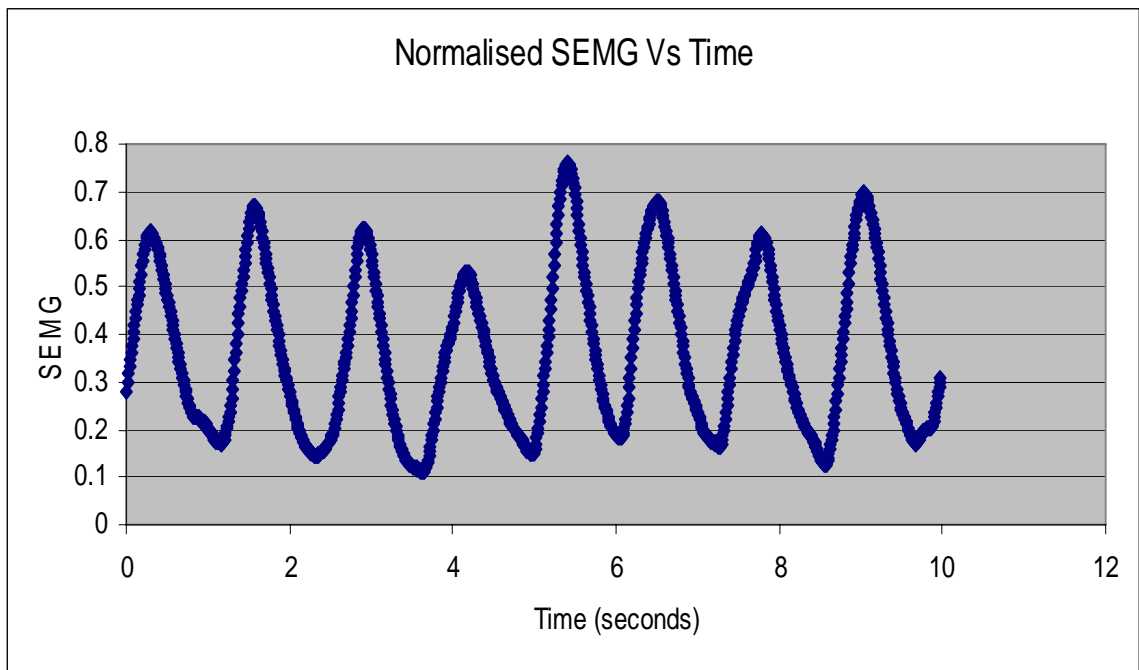


Figure 4.9: Plot of RMS SEMG Vs time for 0.8 Hz. The raw SEMG was subjected to RMS window of length 10 and was filtered with 2 Hz ButterWorth filter.

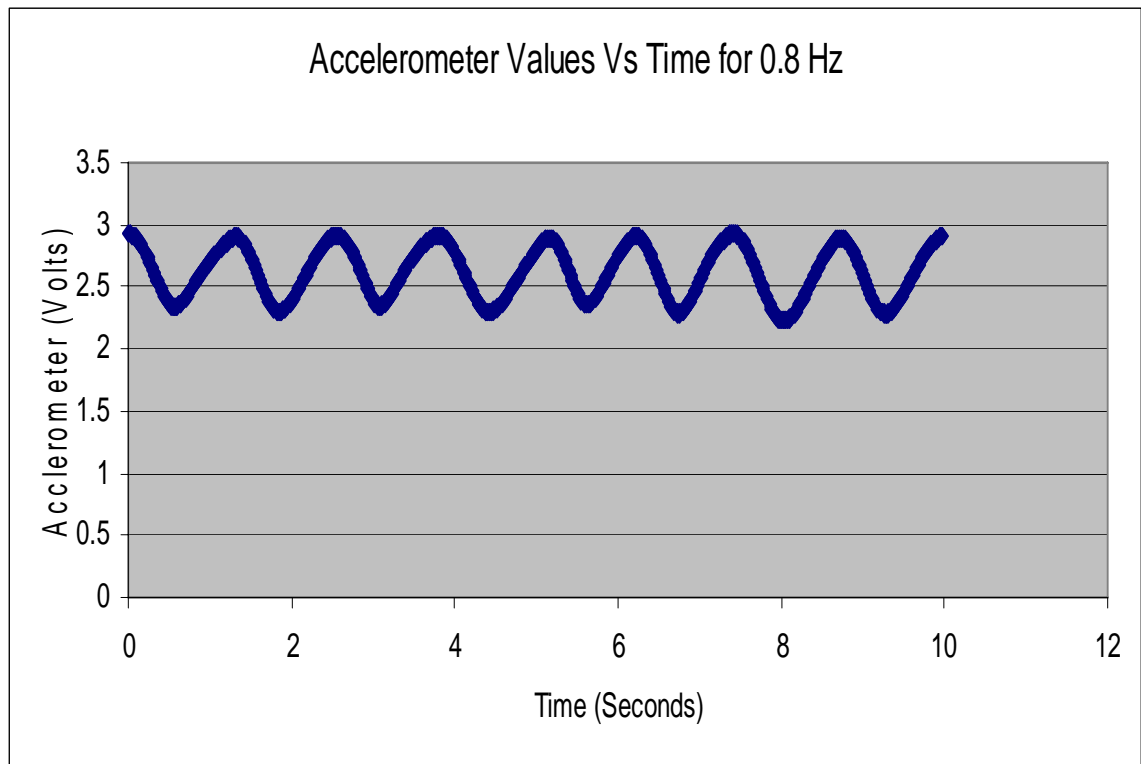


Figure 4.10: Plot of Accelerometer values plotted against time. The accelerometer was mounted on the proximal metacarpophalyngeal joint of the index finger. The accelerometer values increases as finger moves from extensor to flexor.

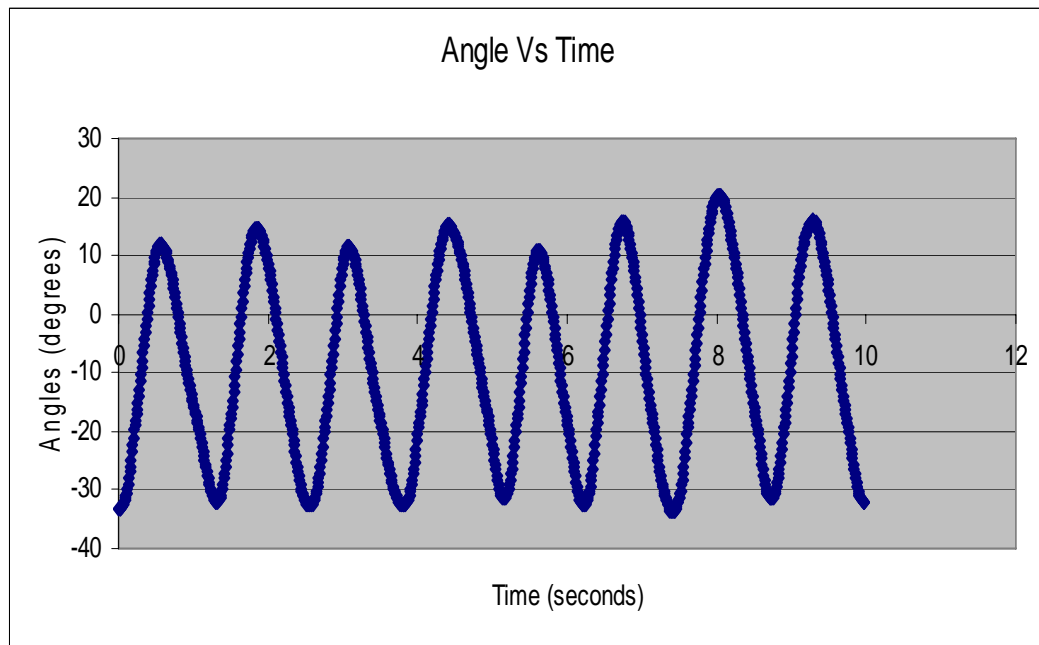


Figure 4.11: Corresponding plot of calculated angles from accelerometer values when the subject performed rhythmic flexion and extension of index finger at 0.8 Hz.

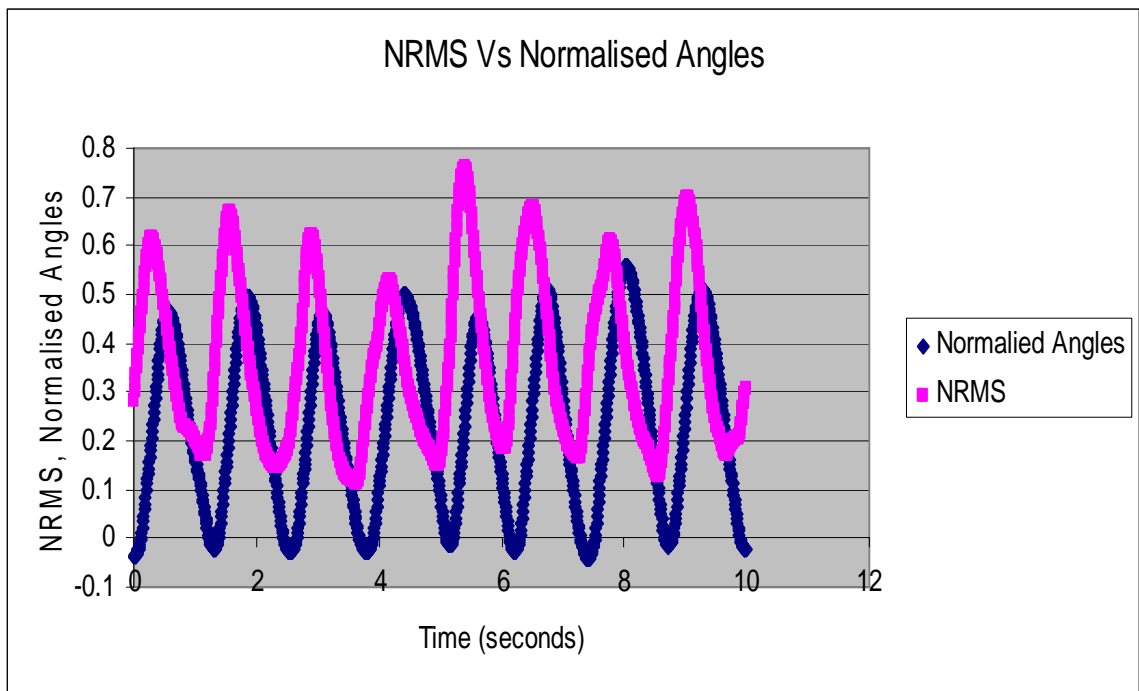


Figure 4.12: Plot of NRMS and normalized angle plotted against time for 0.8 Hz. The average value of SEMG increases with increase in the velocity of rotation.

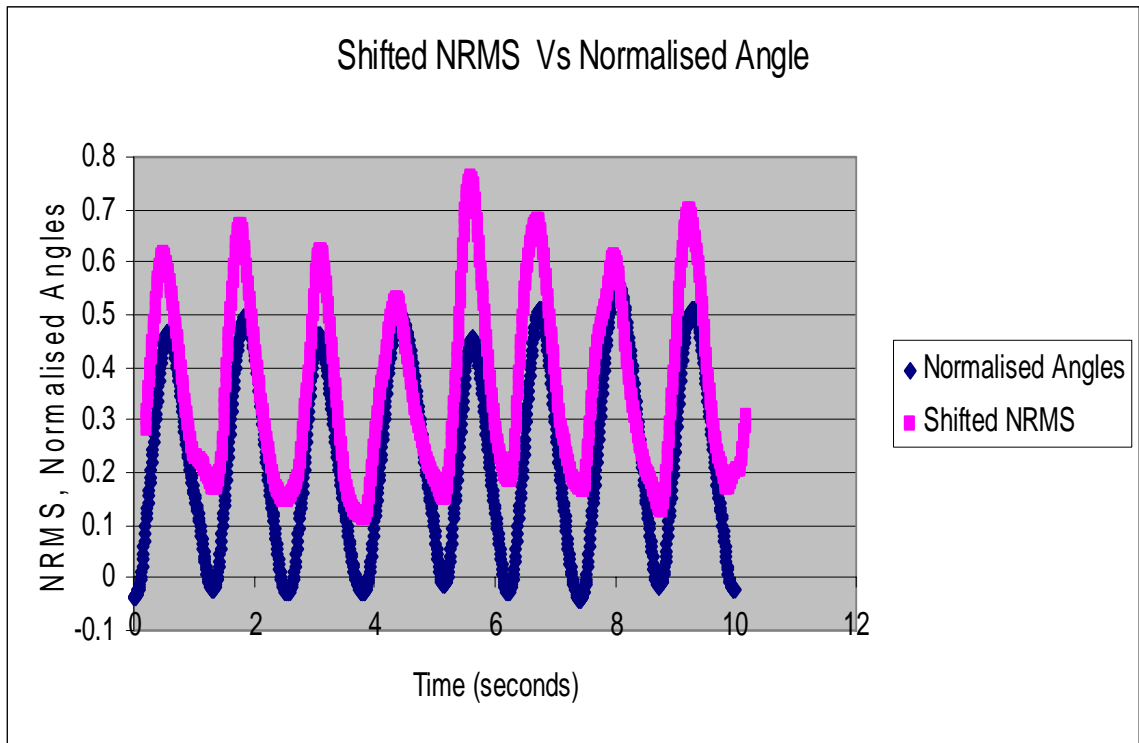


Figure 4.13: Plot of shifted NRMS and normalized angles plotted against time for the rotation of finger at 0.8 Hz.

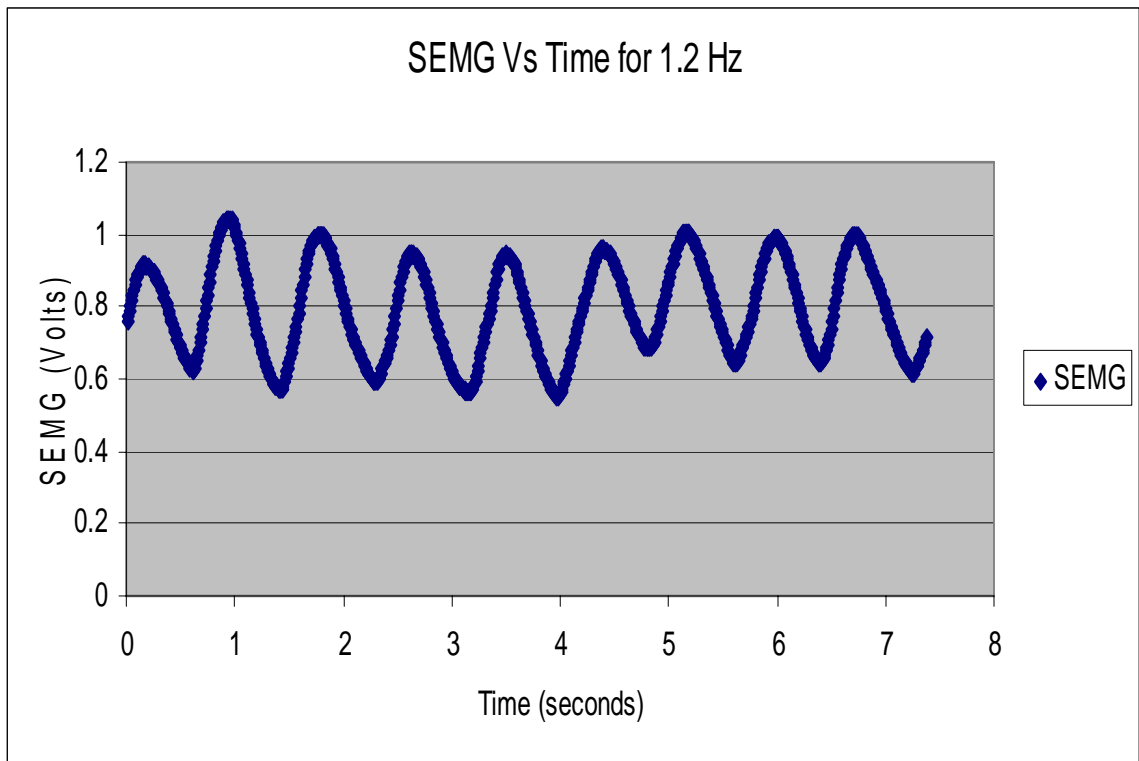


Figure 4.14: Plot of SEMG Vs time for the rotation of the index finger at 1.2 Hz.

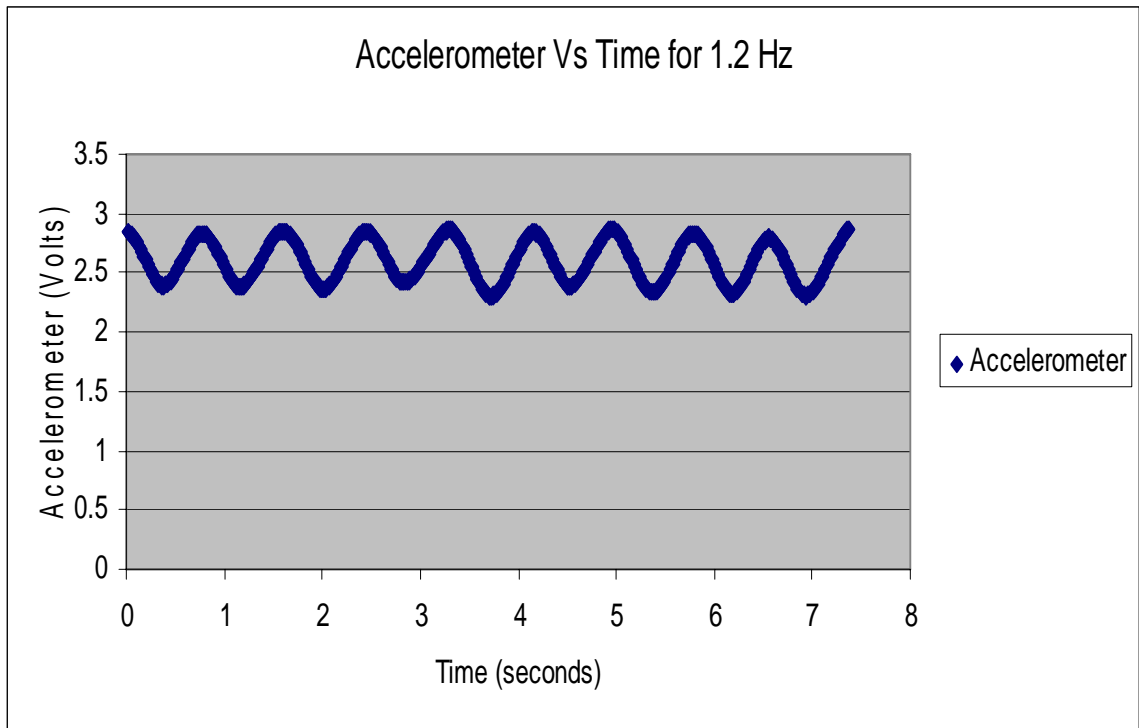


Figure 4.15: Plot of accelerometer voltages against time when the subject is rotating the finger at 1.2 Hz.

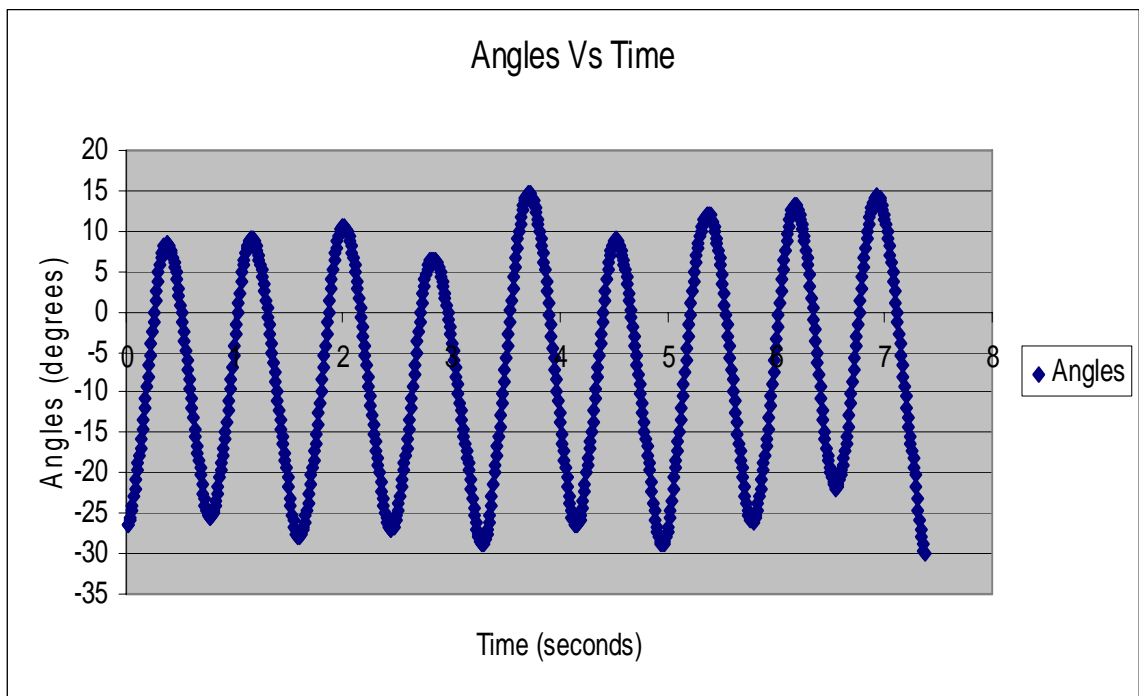


Figure 4.16: Plot of calculated angles from the accelerometer voltages when the subject performed rhythmic flexion and extension of index finger at 1.2 Hz.

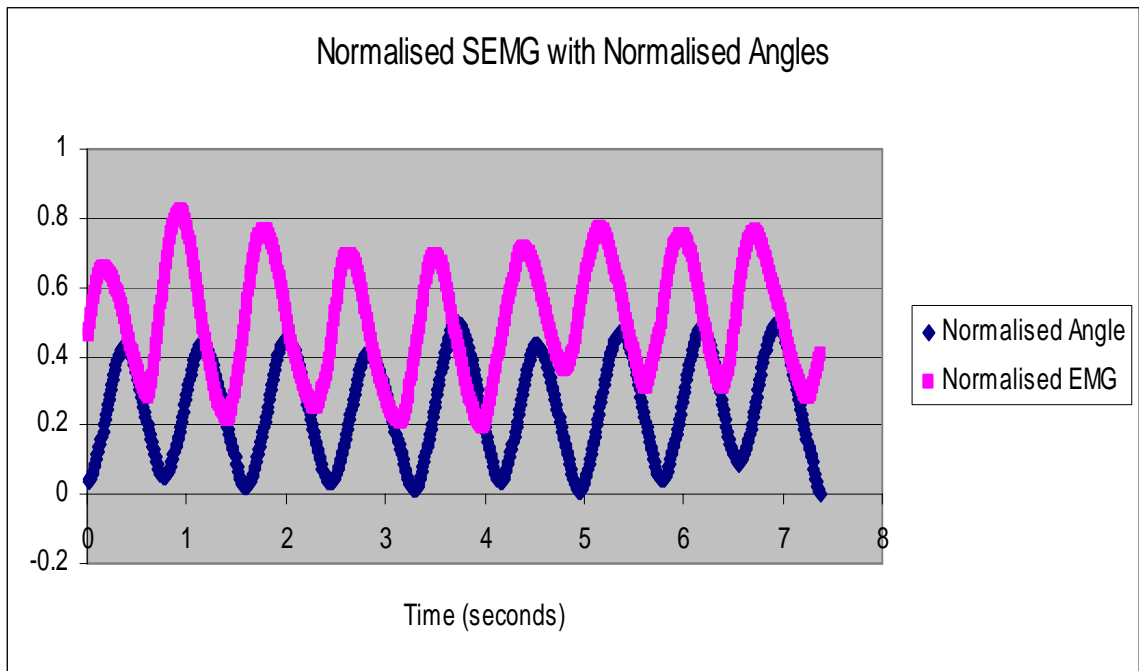


Figure 4.17: Plot of NRMS and normalized angles with respect to time when the subject performed rhythmic flexion and extension of index finger at 1.2 Hz. The maximum value of SEMG with respect to the maximum angles, indicating the effect of velocity on the SEMG.

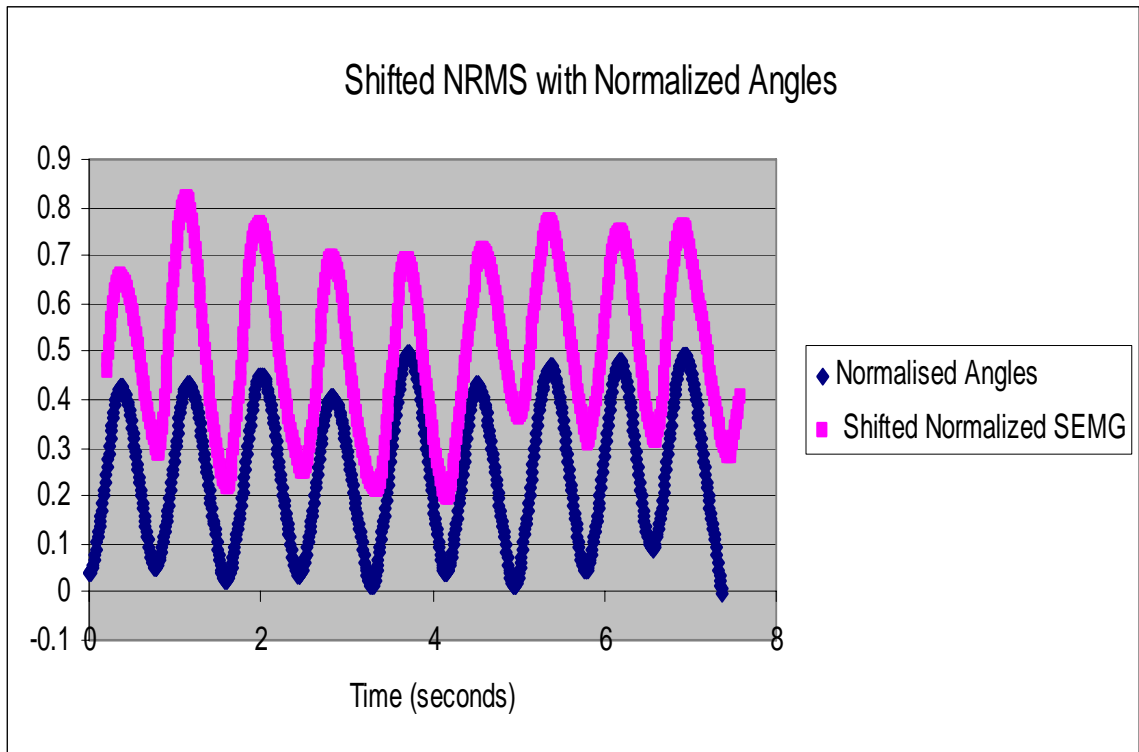


Figure 4.18: Shifted NRMS and normalized angles plotted against time when the subject performed flexion and extension of finger at 1.2 Hz.

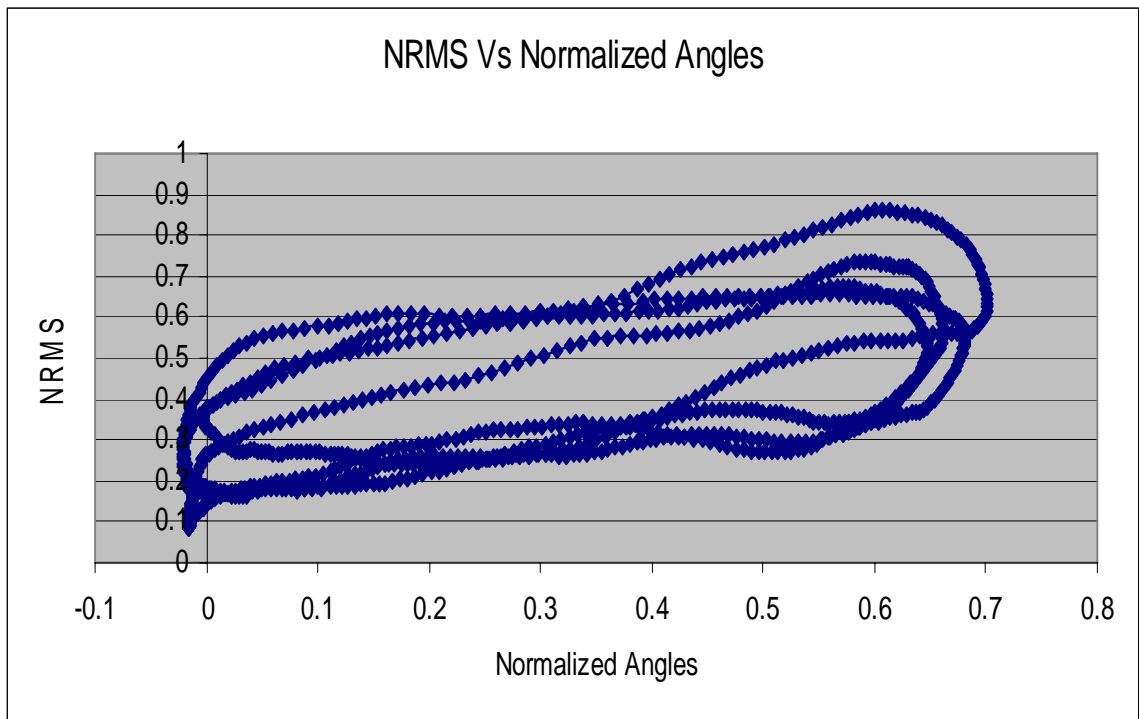


Figure 4.19: NRMS plotted against normalized angles for 0.4 Hz speed of flexion and extension of index finger. Upper part of the curve indicates the SEMG when the subject moved finger from flexor to extensor region and lower part represents SEMG when the finger was moved from extensor to flexor region.

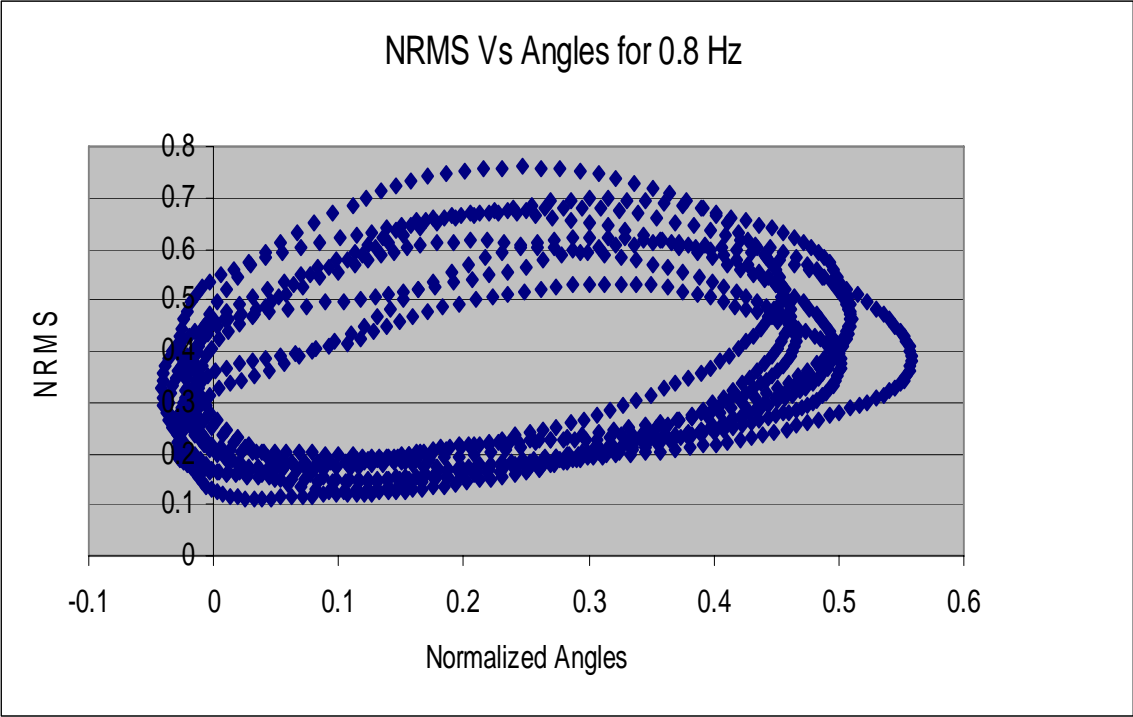


Figure 4.20: NRMS plotted against normalized angles for the rotation speed of 0.8 Hz.

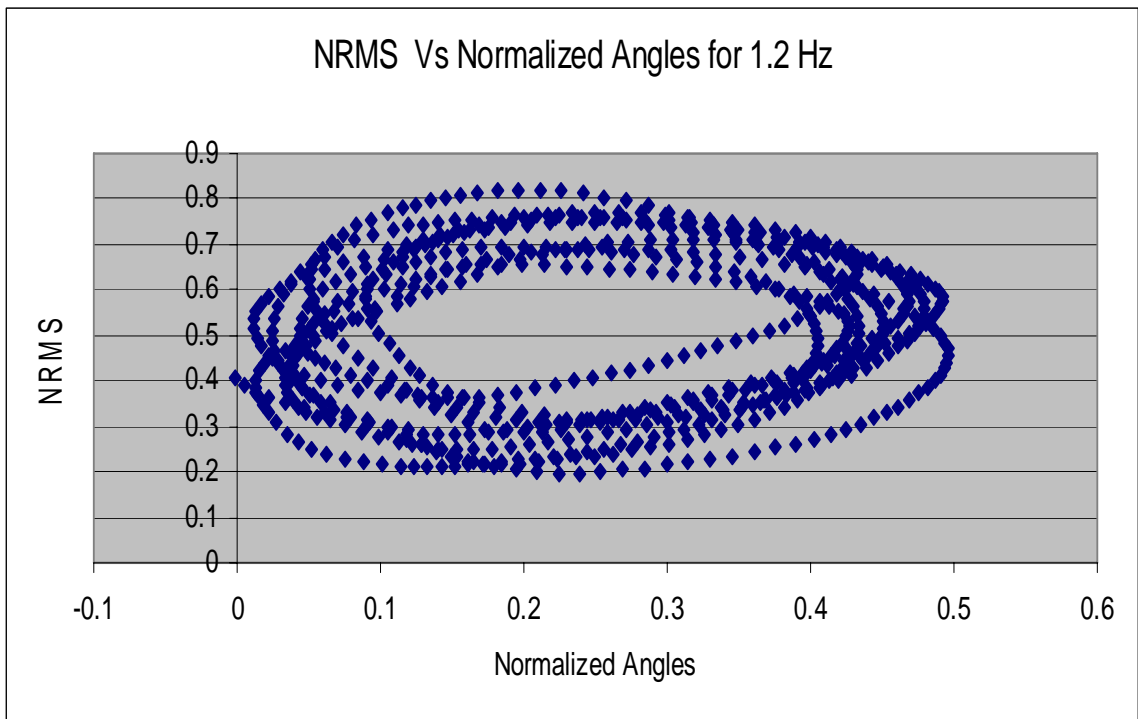


Figure 4.21: NRMS plotted against normalized angles for the rotation speed of 1.2 Hz.

well as predicted angle. Data from six subjects were used to train the neural networks. The neural networks were trained for different training algorithms, with different hidden layers and different training functions. Two committees were formed for each speed, one for flexion and one for extension. These committees were recruited based on the evaluation of networks by data from two new subjects. Best five networks were selected for the recruitment in the committee. Data from nine new subjects were used for the performance evaluation of the committees. The committee was subjected to evaluation by data from each subject. A difference was found between each output predicted by the member of the committee and the average output predicted by the committee. Based on these values, two outliers were eliminated and an average of the remaining three networks was taken as the output of the committee. The angles predicted by the committee were used for finding the RMS errors between the predicted and actual angles. Table 4.1 shows the RMS errors for each subject at different speeds.

4.3 Statistical Analysis

An anova performed on the RMS errors showed significant statistical difference between errors when subject performed finger rotation at 1.2 Hz, and errors when subject performed finger rotation at 0.8 Hz and 0.4 Hz ($p < 0.05$). Appendix B shows detail analysis of the anova performed. An anova was also performed between errors when the finger was rotating from flexion to extension (up) and when the finger was moving from extension to flexion (down). The results show a significant difference in the errors ($p < 0.05$) (Appendix B).

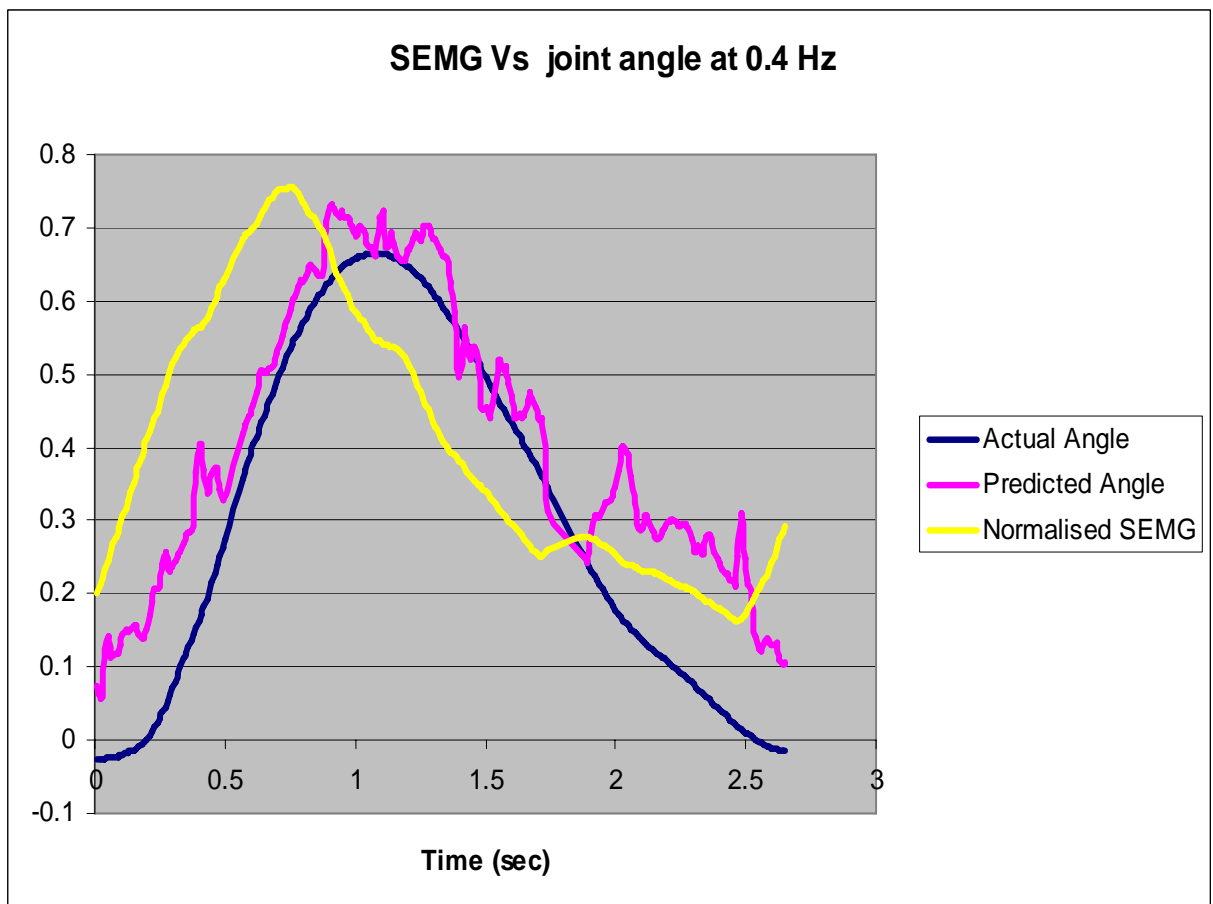


Figure 4.22: NRMS, actual normalized angle and predicted normalized angle plotted against time for one cycle of rotation of index finger at 0.4 Hz.

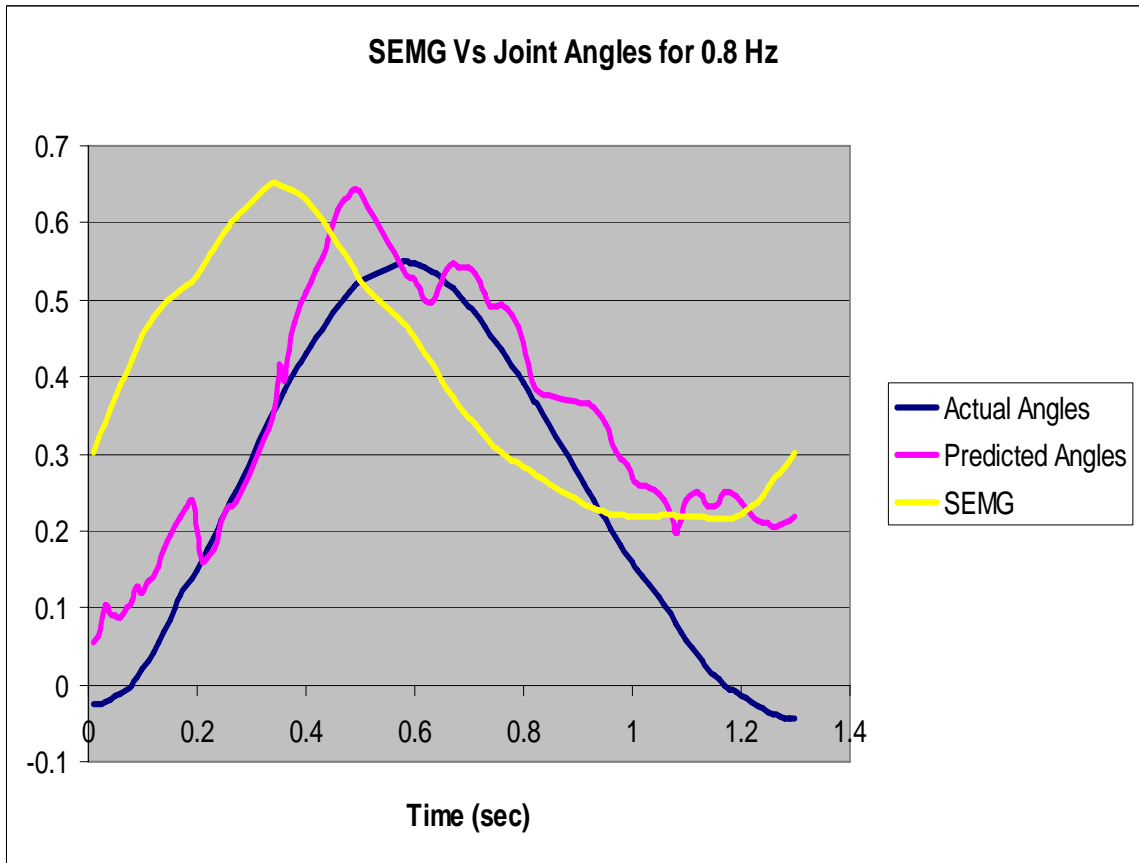


Figure 4.23: NRMS, Actual normalized angles and Predicted angles plotted against time for one cycle of rotation of index finger at 0.8 Hz.

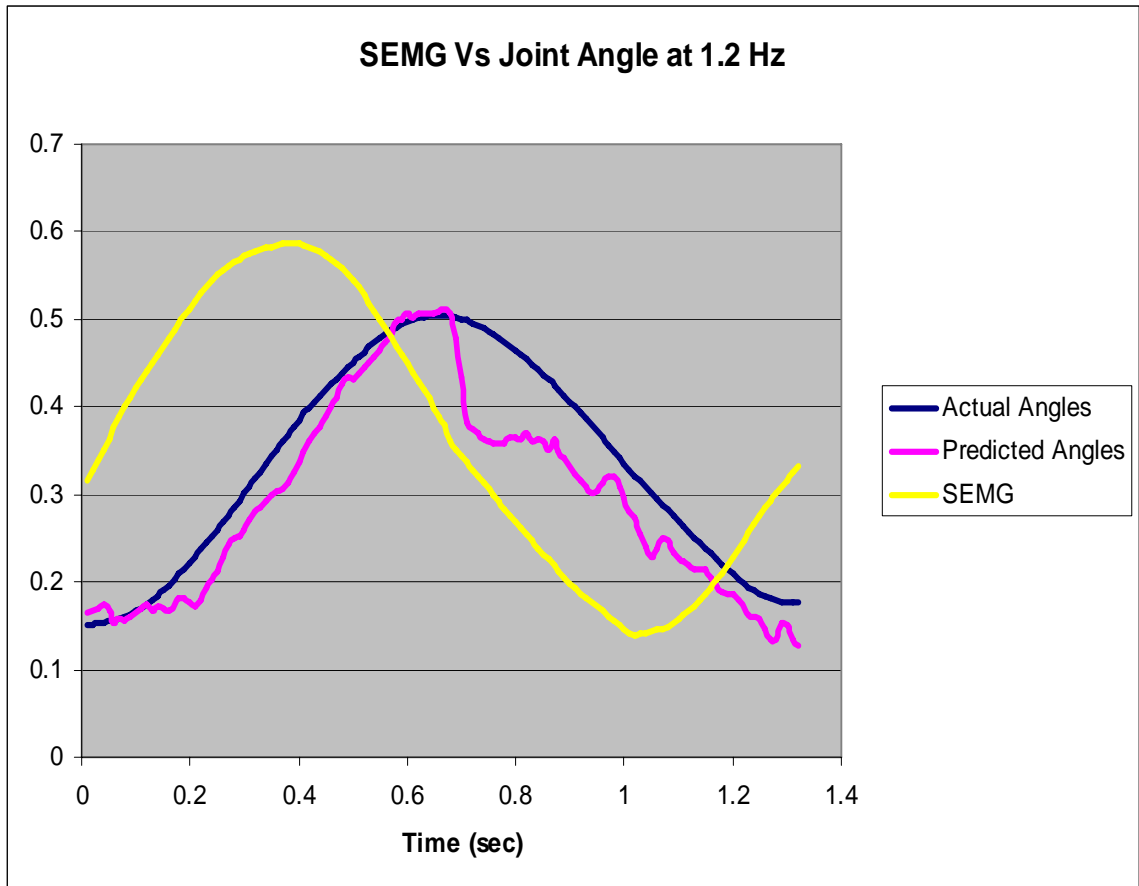


Figure 4.24: Plot of NRMS, Actual angle and Predicted angle with respect to time for the rotation of index finger at 1.2 Hz. The errors associated with the higher speed are less as compared to the errors associated with medium and lower speeds.

Table 4.1: RMS errors for the prediction of the joint angle by CNN.

Subjects	RMS Errors					
	Slow Up	Slow Down	Medium Up	Medium Down	Fast Up	Fast Down
1	0.16517	0.14783	0.13452	0.158157	0.0990	0.09123
2	0.13670	0.13549	0.071392	0.104468	0.0769	0.09855
3	0.16141	0.148953	0.09492	0.149022	0.0642	0.09311
4	0.13017	0.089692	0.054939	0.119592	0.035618	0.07087
5	0.12799	0.15293	0.116979	0.151545	0.10848	0.11014
6	0.19030	0.2724	0.17490	0.176401	0.14293	0.09460
7	0.11829	0.12253	0.057852	0.1814	0.058993	0.07262
8	0.1227	0.214634	0.192727	0.25016	0.124073	0.15047
9	0.17292	0.179743	0.085727	0.2304	0.0527	0.10209
Mean	0.14729	0.162689	0.1093	0.169016	0.0847	0.09819
SD	0.02561	0.05386	0.049699	0.047424	0.035857	0.02339

CHAPTER V

DISCUSSION

The present study has demonstrated the use of the SEMG from EDS in tracking the index finger movement at different speeds. The potential application of this study includes the biocontrol of anthropomorphic telemanipulators and VR environments. The study was also first of its kind to demonstrate the use of Committee Neural Networks (CNN) in a control prediction problem. The SEMG decreased as the finger moved towards the thumb and correspondingly increased as the finger moved away from the thumb (Figures 4.7,4.12,4.17), thus supporting the first alternate hypothesis of the study that there exists a definite relationship between the surface EMG of EDS during the flexion and extension of the index finger (failed to accept the first null hypothesis). CNNs well predicted the angle using the SEMG signals (RMS errors 0.128, Table 4.1, Figures 4.22-4.24). Therefore, it can be said that the SEMG from the EDS along with neural networks can be used for the prediction of the joint angle of rotation of the index finger in extensor as well as the flexor region.

The overall RMS error for the prediction of the joint angle by CNN was 0.128547 ± 0.051054 (Table 4.1) which was considerably less than 0.2. Hence, the results support the second alternate hypothesis that SEMG from EDS along with CNNs can be used to predict the joint angle of finger during flexion and extension at varying speeds

(failed to accept the second null hypothesis). The predicted angle followed the actual angle measured by the accelerometer for all the three speeds (Figures 4.22, 4.23 and 4.24). The errors in the present study were less than the previous studies (<0.2) conducted by Suryanarayan and Reddy (1997) for prediction of elbow joint angles during flexion and extension of the arm in vertical plane, and by Devavaram (2003) on the prediction of the joint angle of the index finger using SEMG from Flexor Carpi Ulnaris (average error of 4.79° in a range of 20° which translates to RMS error of 0.24). Devavaram (2003) trained one committee for each individual subject. Moreover, the testing data as well as training data were derived from the same subject. In the present study, same CNNs were used for all subjects. In addition, the training data were obtained from different subjects and the testing data were obtained from entirely different subjects. The present investigation used two committees for each speed as compared to the use of one committee for every subject by Devavaram (2003). This decreased the computational complexities and time required for calibration and prediction of the angle. Another study conducted by Koo and Mak (2005) on the feasibility of EMG driven neuromusculoskeletal model for prediction of dynamic movement of the elbow showed the error of $34.49^\circ \pm 6.05^\circ$ for the unloaded elbow flexion protocol and $22.27^\circ \pm 4.07^\circ$ for the unloaded voluntary elbow extension protocol. Therefore, the present study marks a very prominent improvement in the use of SEMG for direct biocontrol problems.

The RMS errors were less during extension as compared to flexion (Table 4.1). The average RMS error when the finger was extending was 0.11377 ± 0.045217 which was less as compared to the average errors when the finger was flexing ($0.1422 \pm$

0.0531). This shows that EDS is better in predicting the angle during extension when compared to flexion. Such trends were also observed by Suryanarayanan and Reddy (1997) where they used SEMG from flexor muscle (biceps) for the prediction of the elbow joint angle and the errors were high during extension as compared to flexion. Perhaps, the use of SEMG from extensor muscle during extension and flexor muscle during flexion may improve the performance of the system.

There exists a complex relation between the SEMG, angle of rotation, velocity of rotation and direction the rotation. The SEMG increases with the velocity and changes according to the joint angle. Increase in velocity increases the collective firing of the underlying neurons and therefore, increased activity and increased SEMG. SEMG have higher peaks with respect to the angle for 1.2 Hz as compared to other two speeds (Figures 4.4, 4.9 and 4.14). The committees were better in predicting the joint angle at the faster speed as compared to the slower speeds (Table 4.1). The average RMS error at 1.2 Hz was 0.091476 ± 0.03103 while the average RMS errors at 0.8 Hz and 0.4 Hz were 0.13917 ± 0.05624 and 0.1549 ± 0.0416 respectively. The complex relation between the SEMG and the angle of rotation is highlighted by the fact that SEMG leads over joint angles for all the three speeds (Figures 4.4, 4.9 and 4.14). The reason for this behavior of SEMG can be traced to the origin of SEMG. EMG is a result of the electrical activity of the muscle and it represents the collective action potential of the neurons at a particular instance of time. The resting potential of a cell is -70mV. This resting potential is established by the active transport of Na^+ and K^+ ions in the cell. The cell contraction takes place when the action potential reaches 35mV. The change in the action potential is

caused by the nervous stimulus. This causes the cell to contract and the collective contraction of the cells causes a muscle to contract. A lot of chemical and mechanical process takes place after the generation of action potential, which delays the contraction of the muscles by a few milliseconds. A delay of 0.2 seconds would synchronize the SEMG and angle of rotation (Figures 4.5, 4.10 and 4.15). SEMG from EDS also depends on the direction of the rotation of the index finger. For a given joint angle, the SEMG generated when the finger was extending, was higher as compared to when the finger was flexing. This led to the hysteresis. The plots (Figures 4.19 to 4.21) show a hysteresis with the upper part of the curve representing the SEMG when the finger was extending and the lower part of the curve representing the SEMG when the finger was flexing. This phenomenon can be explained by the fact that the muscle has to work against the gravity while going away from the thumb as a result the effort is more, resulting in higher SEMG. The hysteresis was the main reason for choosing different neural networks for predicting the joint angle during extension and flexion.

The results of the CNNs depend on several factors, including the choice of the muscle, quality of the signal and signal processing algorithms.

EDS was chosen for three reasons:

1. Previous studies for the tracking of index finger movement using SEMG were conducted using the FDS muscle (Devavaram, 2003). The results showed a lot of scope for improvement. Preliminary results conducted on the EDS showed very encouraging results.
2. EDS is one of the most superficial muscles on the forearm. Being a superficial

muscle, it was very easy to palpate.

3. EDS is directly connected to the index finger. This reduced the interference of SEMG from other muscles during the rotation of index finger.

The fidelity of the EMG signal acquired at the source dictates the information content of the signal, and its subsequent effectiveness in prediction of the joint angle. It is desirable to acquire the SEMG signal with maximum information content and least noise interference due to motion artifacts or power line interference. There were two main sources of motion artifact: one from the interface between the detection surface of the electrode and the skin, the other from movement of the cable connecting the electrode to the amplifier. Both of these interferences can be minimized by proper placement of electrodes and employing a proper circuitry. Placement of electrodes plays a very important role in acquisition of the SEMG signals. Proper placement of electrodes insures the maximum amplitude of the SEMG due to desired muscle group with maximum signal to noise ratio. The electrodes used for the acquisition of the SEMG were silver/silver chloride electrodes with inter-electrode spacing of 21 mm. The amplitude of the SEMG is directly proportional to the inter-electrode distance (Basmijian, 1985). For maximum amplitude, the inter-electrode distance should be more. Conversely, if the inter-electrode distance is more, the chances of cross talk increase. Hence, there should be a trade of between inter-electrode distance and desired amplitude. The experiments have shown that an inter-electrode spacing of 21 mm gives sufficient amplitude of the detected SEMG signal from EDS. Apart from inter-electrode distance, other factors such as employing conductive surface between the skin and the electrode, removal of dead dermis from the surface and

placement of the electrode parallel to the muscle, are also responsible for the greater amplitude and hence maximum signal to noise ratio of the SEMG. Care was taken while placing the electrodes that most of the factors mentioned above were satisfied.

The reference electrode was placed on the bony surface of the metacarpophalangeal joint of the little finger. This bone was the best available location for the placement of reference electrode, since it is farthest from the index finger and the activity of the EDS has little effect on the movement of little finger.

The other problem which was encountered while measuring the SEMG was that of capacitance coupling at the input of the differential amplifier. The source of the problem was the high input impedance of the differential amplifier. The problem was solved by reducing the distance between the differential amplifier and the location of the measurement of the SEMG.

The instrumentation system used for the data acquisition is the other important factor which governs the signal to noise ratio of the system. A two stage, two channels pre-amplifier was specially designed for the present study. The first stage of the preamplifier was a bipolar differential precision instrumentation amplifier. The two important criteria for judging an amplifier are its efficiency and impedance. The efficiency of the amplifier refers to the amount of power consumed by the amplifier which should be as low as possible. High input impedance ensures that the input will not overload the source of the signal and reduce the strength (voltage) of the signal by a substantial amount. The SEMG signal measured at the source was of the order of μV . Therefore, for keeping intact the fidelity of the measured signal, the pre-amplifier

required very high input impedance. The input impedance of the pre-amplifier designed was $>2M$ and the power consumed was less than $1mW$.

The gain of the pre-amplifier was chosen to be 4000 to convert the μV signal into an mV signal. The output of the pre-amplifier was isolated from the subject by an isolation amplifier. This ensured the safety of the subject from direct contact with power line. The signal was then fed to an amplifier with an inbuilt notch filter and bandpass filter. The notch filter prevented any distortion of the signal by 60 Hz noise. The power density function of the SEMG signals has very little contributions outside the range of 20-450 Hz (Basmijian, 1985). Therefore, the higher and lower cutoff frequencies for the bandpass filter were chosen as 300 and 30 Hz respectively. Frequencies lower than 30 Hz mainly constitute the noise due to motion artifacts and frequencies above 300 Hz contribute to the environmental noise. The digitization of the signal was done by a 16 bit A/D converter with the measurement range of $\pm 10 V$. Therefore, the resolution of the system was 0.0048 V. This made the resolution of the overall system to be $0.05 \mu V$. The signal was sampled at 1000 Hz. The minimum sampling rate required for the satisfaction of Nyquist criteria was 600 Hz. The sampling rate satisfied the Nyquist criteria and therefore, prevented any aliasing.

The raw EMG has a random component which is present because of the large number of neuron firing at any time, and is unpredictable. This random component makes the processing of the raw EMG unsuitable. Several different techniques have been used for the processing of raw EMG signals, including rectification of the signal and then smoothing of the signal using a low pass filter. This process is called as linear envelop

detection. Another method used for the envelop detection, which was used in this project for the processing of SEMG is Root Mean Square (RMS) value. RMS gives the overall shape of the SEMG signal pattern. The shape and the amplitude of the envelope gave an account of the activity performed by the muscle. The amplitude of the envelope of SEMG for the rotation of the index finger can be related to the velocity and the force applied during the rotation. The RMS of the SEMG was found by a moving window of fixed length. The length of the window determines the computing time and the resolution of the system. As the length of the window (>200) increases, the computation time decreases. However, the resolution of the system also decreases. Similarly, decreasing the length of the window (<5) will increase the resolution but will increase the computation time. The tradeoff between the resolution and the computation time was achieved by using the window length of 10. The RMS SEMG still had some fluctuations which were making the model unstable. These fluctuations were removed by further low pass filtering the RMS SEMG using a 2nd order ButterWorth low pass filter.

The SEMG varies with various factors such as time, temperature, humidity. The SEMG of the same person may be different at different times. Therefore, it is very necessary to normalize the SEMG signal so that all the data sets can be evaluated based on a single platform. There are many ways of normalizing a signal. The present investigation used normalization with minimum and maximum SEMG of the subject recorded during the calibration process. This assumed a linear relation between SEMG and the angle of rotation. This enabled the data sets of different individuals to be evaluated on the same platform.

The intelligent system developed for this study acts like a black box model with SEMG as the input and the predicted angle as the output. The neural networks were trained in MATLAB using different training functions, different training algorithms, different hidden layers and different neurons in the hidden layer. It was observed that the training algorithm ‘trainrp’ works best for this problem; therefore, all the networks used in the committee were trained using this training function. In present study, the number of hidden layers was limited to two. As the number of hidden layer increases, the network has more weights to describe the relation between input and output. However, increase in the number of hidden layer also increases the complexity of the network and considering that the network would be used for the real time, the hidden layers were limited to two.

Biocontrol using SEMG provides unrestricted finger movements. Currently available systems are worn externally and restrict the motion of the fingers. Other devices like Magnetic Trackers require isolation. The present study visualizes a significant step forward for dynamic biocontrol of telemanipulators and VR environments using SEMG signals. The applications of the present study are telemanipulation, video games industry and in real world simulation. The present study also demonstrates the use of CNNs for control related prediction problems. One of the drawbacks of the study was that, it didn't consider the effect of muscle loading. An improved algorithm and intelligent system would be required for the prediction of the joint angle when the muscle is loaded. With further improvements, the technique can be developed into an ideal and synergistic control for telemanipulators and VR environments.

CHAPTER VI

CONCLUSION AND FUTURE WORK

6.1 Conclusion

The conclusions of the study were:

1. SEMG signals were successfully measured from the EDS during the flexion and extension of index finger at three different speeds.
2. ANNs were trained for different speeds for the prediction of the joint angle from the extracted parameters.
3. CNNs, comprising of five best networks were recruited for the prediction of the joint angle.
4. Performance of the system was evaluated by calculating the RMS error between the measured angle and the predicted angle. The average error was found to be 0.128547 ± 0.051054 .
5. The results of the study concluded that we fail to accept both the null hypotheses of the study. Results support the alternate hypotheses that:-
 - There exists a definite relation between the SEMG from Extensor Digitorum muscle (EDS) and the joint angle of the finger movement at various speeds.
 - SEMG along with Committee Neural Networks (CNN) can be used for predicting the joint angle of the finger movement at various speeds

6.2 Recommendations for the future work

1. The study did not take into account the loading effect of the muscle. More investigations can be carried out to study the effect of loading on the SEMG when the finger is rotating at various speeds.
2. The study can be extended to the movement of the other fingers along with the index finger.
3. SEMG from Flexor muscle can be combined with SEMG from EDS for better prediction of the joint angle of the finger during flexion and extension.
4. The study can be integrated with similar studies on the static measurement of the SEMG for control problems for integrating the system for static as well as dynamic movement of the finger.
5. A hybrid intelligent system can be developed for the better prediction of the angle, involving CNNs and Fuzzy Logic.

REFERENCES

- Abel EW, Zacharia PC, Forster A, Farrow TL, "Neural Network Analysis of the EMG Interference Pattern," [Medical Engineering and Physics](#), 18(1): 12-17, 1996.
- Basmajian JV, "Muscles Alive: Their Functions Revealed by Electromyography," the Williams and Wilkins Company, Baltimore, 1974.
- Bilodeau M, Arsenault AB, Gravel D, Bourbonnais D, "Time and Frequency Analysis of EMG Signals of Homologous Elbow Flexors and Extensors," *Med. Biol. Eng. Comput.*, 30(6): 640-644, 1992.
- Burdea G, Langarana N, "Virtual Force Feedback: Lessons, Challenges, Future Applications," *Advances in Robotics*, 42(1): 41-47, 1992.
- Cromwell L, Weibell FJ, Pfeiffer EA, "Biomedical Instrumentation and Measurements," Prentice Hall Inc., New Jersey, 1980.
- Das A, Reddy NP, Narayanan J, "Hybrid Fuzzy Logic Committee Neural Networks for Recognition of Swallow Acceleration Signals," *Computer Methods and Programs in Biomedicine*, 64: 87-99, 2001.
- De Luca CJ, "Surface Electromyography: Detection and Recording," Delsys Inc, Boston, MA, 2002.
- De Luca CJ, "Physiology and Mathematics of Myoelectric Signals," *IEEE Trans. Biomed. Eng.*, 26: 313-325, 1979.
- Devavaram A, "Committee Neural Networks for Tracking Finger Joint Movements for VR Application," Master's Thesis, The University of Akron, 2003.
- Dipietro L, Sabatini AM, Dario P, "Evaluation of an Instrumented Glove for Hand-Movement Acquisition," *Journal of Rehabilitation Research and Development*, 40(4): 179-190, 2003.
- Duchene J, Goubel F, "Surface Electromyography during Voluntary Contraction: Processing Tools and Relation to Physiological Events," *CRC. Crit. Rev. Biomed. Engr.*, 21(4): 313-397, 1993.

- Fakuda O, Tsuji T, Kaneko M, Otsuka A, "A Human Assisting Manipulator Teleoperated by EMG Signals and Arm Motions," *IEEE Transactions on Robotics and Automation*, 19(2): 210-221, 2002.
- Farry K, Walker ID, Baraniuk RG, "Myoelectric Teleoperation of a Complex Robotic Hand," *IEEE Transactions on Robotics and Automation*, 12(5): 775-787, 1995.
- Gibson JJ, "The Senses Considered as Perceptual Systems," Boston:Houghton Mifflin, 1966.
- Gibson JJ, "The Ecological Approach to Visual Perception," Boston:Houghton Mifflin, 1979.
- Gupta V, Reddy NP, Canilang EP, "Surface EMG Measurements at the Throat during Dry and Wet Swallowing," *Dysphagia*, 11: 173-179 ,1996.
- Gupta V, Reddy NP, "Control of Anthropomorphic Teleoperator Finger and Wrist Models Using Surface Electromyogram," Doctoral Dissertation, the University of Akron, 1997.
- Guyton AC, "Textbook of Medical Physiology," W.B. Saunders Company, Philadelphia, 1971.
- Hertz J, Krogh A, Palmer R, "Introduction to the Theory of Neural Computation," 1991.
- Jacobsen S, "Design of the Utah/MIT Dextrous Hand," *Proc. 1986 IEEE International Conference on Robotics and Automation*, San Fransisco, April 7-10, 1986.
- Jerard RB, Williams TW, Ohlenbusch CW, "Practical Design of an EMG Controlled Above Elbow Prosthesis," *Proc. Conf. Engineering Devices for Rehabilitation*, Boston, MA, 73-73, 1974.
- Kato E, Okazaki H, Iwanami K, " Electropneumatically Controlled Hand Prosthesis Using Pattern Recognition of Myo-electric Signals," *Digest 7th ICMBE* , 367-367, 1967.
- Kearney RE, Hunter IW, "System Identification of Human Joint Dynamics," *CRC Critical Review Biomed. Engr.*, 18(1): 55-87, 1990.
- Kelly MF, Parker PA, Scott RN, "Application of Neural Networks to Myoelectric Signal Analysis: A Preliminary Study," *IEEE transactions on Biomedical Engineering*, 37(3): 221-229, 1990.

Kenemans JL, Molenaar PCM, Verbaten MN, “ Models for Estimation and Removal of Artifacts in Biological Signals,” Digital Biosignal Processing (ed: Weikunat R.), Elsevier Science Publishers BV, The Netherlands, 213-250, 1991.

Koo KK, Mak AFT, “Feasibility of using EMG Drive Neuromusculoskeletal Model for Prediction of Dynamic Movement of Elbow,” Journal of Electromyography and Kinesiology ,15: 12-26, 2005.

Merletti R, LoConte R, “Advances in Processing of Surface Myoelectric Signals: Part I,” Medical Biological Engineering and Computing, 33(3): 362-372, 1995.

Laffey JG, Tobin É, Boylan JF, McShane AJ, “Assessment of a Simple Artificial Neural Network for Predicting Residual Neuromuscular Block,” British journal of anaesthesia , 90(1): 48-52, 2003

Mitchell M, “[Machine Learning](#),” McGraw Hill Companies, Inc., Section 4.1.1, 82, 1997.

Palmer JB, Holloway AM, Tanaka E, “Detecting Lower Motor Neuron Dysfunction of the Pharynx and Larynx with Electromyography,” Archives of Physical Medicine and Rehabilitation, 72: 214-218, 1991.

Palreddy S, “Computer Aided Diagnosis Using Neural Network Models: Classification of Dysphagic Patients”, Masters Thesis, The University of Akron, 1993.

Pashtoon NA, “IIR Digital Filters,” Handbook of Digital Signal Processing: Engineering Application (ed: Elliot E. F), Rockwell International Corporation, 289-355, 1987

Perlman AL, Luschel ES, DuMond CE, “Electrical Activity from Superior Pharyngeal Constrictor during Reflexive and Nonreflexive Tasks,” Journal of Speech and Hearing Research, 32: 749-754, 1989.

Prabhu D, Reddy NP, Canilang E, “Neural Networks for Recognition of Acceleration Patterns During Swallowing and Coughing Pattern,” Proceedings of the 16th Annual International Conference on the IEEE-Engineering in Medicine and Biology Society, 1105-1106, 1994.

Rassweiler JA, Binder JC, Frede TB, “Robotic and Telesurgery: Will They Change our Future?,” Current Opinion in Urology,11(3): 309-320, 2001.

Reddy NP, “Redundant Neural Networks for Medical Diagnosis: Applications to Dysphagia Diagnosis,” Intelligent Engineering Systems through Artificial Neural Networks, 5: 699-704, 1995.

Reddy NP, Buch O, "Committee Neural Networks for Speaker Verification," *Computer Programs and Methods in Biomedicine*, 72: 109-115, 2003.

Reddy NP, Gupta V, "Toward Direct Biocontrol Using Surface EMG Signals: Control of Finger and Wrist Joint Models," *Medical Engineering and Physics*, In press, 2006.

Reddy NP, Sukthankar SM, Gupta V, "Virtual Reality in Rehabilitation," *IEEE Workshop on Innovations in Rehabilitation Engineering*, Baltimore, MD, 23-26, 1994.

Ronager J, Christensen H, Fuglsang- Frederiksen A, "Power Spectral Analysis of the EMG Pattern in Normal and Diseased Muscles," *Journal of Neurological Sciences*, 94: 283-294, 1989.

Salchenberger L, Enrique VR, Luz VA, "Using Neural Networks to Aid the Diagnosis of Breast Implant Rupture," [Computers & Operations Research](#), 24(5): 435-444, 1997.

Satava RM, "Virtual Reality, Telesurgery, and the New World Order of Medicine," *Journal of Image Guided Surgery*, 1(1): 6-12, 1995.

Shah EN, Reddy NP, Rothschild BM, "Fractal Analysis of Acceleration Signals from Patients with CPPD, Rheumatoid Arthritis, and Spondyloarthropathy of the Finger Joint," *Computer Methods and Programs in Biomedicine*, 77: 233-239, 2005.

Sheridan TB, "Telerobotics, Automation and Human Supervisory Control, Cambridge," the MIT Press, 1992.

Su, F, Wu WL, "Design and Testing of a Genetic Algorithm Neural Network in the Assessment of Gait Patterns," [Medical Engineering and Physics](#), 22(1): 67-74, 2000.

Sukthankar S, Reddy NP, "Virtual Reality of "Squeezing" using Hand EMG Controlled Finite Element Models," *Proceedings of IEEE EMBS 15th Annual International Conference*, San Diego, CA, 972,1993.

Suryanarayanan S, "An Intelligent System for Surface EMG Based Position Tracking of Human Arm Movements for the Control of Manipulators," PhD dissertation, The University of Akron, 1996.

Suryanarayanan S, Reddy NP, "EMG Based Interface for Position Tracking and Control in VR Environments and Teleoperation," *Presence*,6(3): 282-291, 1997.

Sutherland I, "The Ultimate Display," *Proceedings from IFIP Congress*, Amsterdam, Netherland, 506-508, 1965.

Suzanne M, "Virtual Reality in Medicine,"
http://web.cs.wpi.edu/~matt/courses/cs563/talks/smartin/vr_med.html, 1994.

Tatsuya K, "Multi-Fingered Exoskeleton Haptic Device using Passive Force Feedback for Dexterous Teleoperation," Proceedings of the 2002 IEEE/RSJ Intl. Conference on Intelligent Robots and Systems, Lausanne, Switzerland, 2905-2910, 2002.

Wiener N, "CYBERNETICS or Control and Communications in the Animal and Machine," Cambridge, MA, MIT Press, 1948.

Zajtchuk R, Satava R, "Medical Applications of Virtual Reality," Communications of the ACM, 40(9): 63-63, 1997.

APPENDICES

APPENDIX A

ACCELEROMETER READINGS

Table A-1: The accelerometer voltage output at different angles. The voltage output of the accelerometer during clockwise movement (up) and anticlockwise movement (down)

	Data set-1		Data set-2		Data set-3		
Angle	Up(V)	Down(V)	Up(V)	Down(V)	Up(V)	Down(V)	Mean
-40	2.9977	3.0022	2.9969	3.002	3.0272	3.0301	3.00935
-35	2.9352	2.9461	2.9298	2.9441	2.9634	2.9704	2.948167
-30	2.8731	2.8888	2.867	2.8833	2.832	2.9101	2.875717
-25	2.809	2.8294	2.8061	2.8225	2.8338	2.8494	2.825033
-20	2.7462	2.7722	2.816	2.7689	2.7663	2.7853	2.775817
-15	2.6797	2.7094	2.6815	2.711	2.7019	2.7203	2.700633
-10	2.6174	2.6461	2.6176	2.6482	2.6348	2.6555	2.6366
-5	2.5539	2.5797	2.5524	2.5822	2.5719	2.5868	2.57115
0	2.4865	2.5061	2.4878	2.5153	2.518	2.5162	2.504983
5	2.4434	2.4436	2.4288	2.4495	2.4427	2.4447	2.442117
10	2.3627	2.3707	2.3579	2.3795	2.369	2.3776	2.369567
15	2.2922	2.3012	2.2879	2.3053	2.297	2.3059	2.29825
20	2.2255	2.2327	2.2195	2.2335	2.2254	2.2368	2.2289
25	2.1589	2.1647	2.1542	2.1652	2.1562	2.1675	2.161117
30	2.0912	2.0973	2.0888	2.0994	2.0888	2.0984	2.093983
35	2.0283	2.0315	2.0261	2.0382	2.0235	2.0311	2.029783
40	1.97	1.9681	1.964	1.975	1.9603	1.9674	1.967467
45	1.907	1.9096	1.906	1.9147	1.9016	1.9065	1.907567
50	1.8565	1.8548	1.8508	1.8576	1.8451	1.8493	1.85235
55	1.8003	1.8034	1.8036	1.8169	1.7943	1.7963	1.802467
60	1.7559	1.7577	1.7582	1.7593	1.7472	1.748	1.754383

APPENDIX B

STATISTICAL ANALYSIS

B-1 Student-Newman-Keuls Test for Different Speeds

NOTE: This test controls the Type I experiment wise error rate under the complete null hypothesis but not under partial null hypotheses.

Alpha 0.05
Error Degrees of Freedom 51
Error Mean Square 0.001937

Number of Means 2 3
Critical Range 0.029454 0.0354156

Means with the same letter are not significantly different.

	Mean	N	speed
A	0.15499	18	1 Slow (0.4 Hz)
A			
A	0.13916	18	2 Medium (0.8 Hz)
B	0.09148	18	3 Fast (1.2 Hz)

B-2 Student-Newman-Keuls Test for different directions

NOTE: This test controls the Type I experimentwise error rate under the complete null hypothesis but not under partial null hypotheses.

Alpha 0.05
Error Degrees of Freedom 52
Error Mean Square 0.002431

Number of Means 2
Critical Range 0.0269264

Means with the same letter are not significantly different.

	Mean	N	direction
A	0.14329	27	2 (When the finger is moving up)
B	0.11379	27	1 (When the finger is moving down)

APPENDIX C
IRB APPROVAL



Office of Research Services and Sponsored Programs
Akron, OH 44325-2102
(330) 972-7666 Office
(330) 972-6281 Fax

file

July 18, 2005

Nikhil A. Shrirao
491 Sumner St.
Akron, Ohio 44304

Mr. Shrirao:

The University of Akron's Institutional Review Board for the Protection of Human Subjects (IRB) completed a review of the protocol entitled "*Direct Biocontrol of Telemanipulators and VR Environments Using Non-Invasive Surface EMG and Intelligent Systems*". The IRB application number assigned to this project is 20050705.

The protocol qualified for Expedited Review and was approved on July 15, 2005. The protocol represents minimal risk to subjects and matches the following federal category for expedited review:

(4) Collection of data through noninvasive procedures routinely employed in clinical practice


This approval is valid until July 15, 2006 or until modifications are proposed to the project protocol, whichever may occur first. In either instance, an Application for Continuing Review must be completed and submitted to the IRB.

Enclosed is the informed consent document, which the IRB has approved for your use in this research. A copy of this form is to be submitted with any application for continuation of this project.

Please note that within one month of the expiration date of this approval, the IRB will forward an annual review reminder notice to you by email, as a courtesy. Nevertheless, it is your responsibility as principal investigator to remember the renewal date of your protocol's review. Please submit your continuation application at least two weeks prior to the renewal date, to insure the IRB has sufficient time to complete the review.

Please retain this letter for your files. If the research is being conducted for a master's thesis or doctoral dissertation, you must file a copy of this letter with the thesis or dissertation.

Sincerely,


Sharon McWhorter
Associate Director

Cc: Daniel Sheffer, Department Chair
N. P. Reddy, Advisor
Phil Allen, IRB Chair

The University of Akron is an Equal Education and Employment Institution

APPENDIX D
INFORMED CONSENT

Name of the project: Direct Biocontrol of Telem manipulators and VR environments using Non-Invasive Surface EMG and Intelligent Systems.

Investigator: Nikhil Shirao, Graduate student, Department of Biomedical Engineering, The University of Akron.

Purpose: The purpose of this project is to develop a technique for direct biocontrol of computer model of finger using non-invasive Surface Electromyogram (SEMG). This study is conducted towards the partial fulfillment of the requirements for a Master's Thesis.

Method: One pair of electrodes would be taped to your right/left hand on the posterior side of the forearm. One electrode will be taped over the bony structure of the wrist (reference electrode). An angle-measuring instrument (sensor) would be taped on the index finger. The experiment is divided in two sections. First you will be asked to maintain the finger at three specific locations. The recordings at each location would be taken for 20 seconds. In the second part of the experiment you will be asked to move the finger from complete flexion to full extension at 3 different speeds of 0.5 Hz, 1 Hz and 1.5 Hz. The surface electromyogram and the angle would be recorded at each speed for 20 seconds. Your participation in the study will require approximately 20 to 30 minutes.

Benefits. You should view your participation in this project as providing information for the development of the technique and should not expect any personal gain from your participation to the project.

Risks: There is minimal risk Taping the electrodes to the skin may cause minor skin irritation or discomfort. Also a slight discomfort would be felt while the tape is being removed.

Participation: Participation in the project is entirely voluntary and you will not be penalized in any way if you choose not to participate at any time. You can withdraw from the study at anytime without any penalty. No cost for you will result in your participation in the study.

Compensation: You would not be provided any compensation for the participation in the study.

Confidentiality: All information provided by you will be kept confidential. The data will be coded and only the investigators will use the information. The coding would be destroyed after the completion of the study.

You can obtain information on policy regarding the research and subject's rights by contacting the office of the Institutional Review Board (Office of the Research Services, tel: 330-972-7666) at the University Of Akron. If you have any questions regarding the procedures used in the study, please contact Narender P. Reddy, PhD, at 330-972-6653 for clarification.

Your signature below indicates that you understand the purpose of this study and that you of your own free will agree to participate in this project.

(Participant's Signature)

(Date)